

Real-time Vehicle Relocation and Staff Rebalancing Problem for Electric and Shared Vehicle Systems

Ting Wu^a, Min Xu^{a,*}, Abdelrahman E.E.Eltoukhy^b

^a *Department of Industrial and Systems Engineering, The Hong Kong Polytechnic University, Hung Hom, Hong Kong*

^b *Management Science and Engineering Department, Khalifa University, Abu Dhabi, United Arab Emirates*

Abstract

Vehicle relocation in electric carsharing services is complicated by ad-hoc demand and charging requirement of electric vehicles (EVs). The additional staff rebalancing consideration only exacerbates the complexity as staff scheduling constraints come into play. To tackle this intractability, this study proposes a real-time vehicle relocation and staff rebalancing (RT-VR&SR) problem for one-way electric carsharing services considering the demand uncertainty and practical nonlinear charging profile of EVs. The RT-VR&SR problem aims to determine the strategies of vehicle relocation, vehicle charging, and staff rebalancing in a real-time fashion by maximizing the profit of carsharing operators. We first formulate the RT-VR&SR problem as a Markov Decision Process (MDP). Subsequently, we propose an efficient concurrent-scheduler-based policy for the MDP, under which the action at each decision epoch is determined by dispatching pairs of EVs and staff members in a greedy way for fulfilling unserved orders. Given the nonlinear charging profile, an innovative constrained non-dominated charging strategy (CNCS) is proposed to examine the feasibility of a pair of an EV and a staff member for serving an order. Numerical experiments are conducted to demonstrate the efficiency of the proposed policy as well as the developed methodology and to analyse the impact of staff rebalancing. The results indicate that the proposed policy improves the service level and profitability greatly compared to a decomposition-based benchmark policy, the developed methodology shows a good performance, and ignoring staff rebalancing in the decision making of vehicle relocation could cause the overestimation of service level and profitability. Finally, the effects of the demand dynamism and transport mode for staff rebalancing on the performance of one-way electric carsharing systems are analysed.

Keywords: Electric carsharing; Vehicle relocation; Staff rebalancing; Uncertain demand; Concurrent scheduler-based policy.

* Corresponding author

Tel: +852 2766 6593 Fax: +852 2362 5267 E-mail: xumincee@gmail.com; min.m.xu@polyu.edu.hk (M. Xu)

1. Introduction

Carsharing is an innovative business model that enables customers to access private cars without bearing the costs and responsibilities of owning a car (Kang et al., 2022; Li and Zhang, 2023). The past few decades have witnessed the increasing popularity of carsharing worldwide (Weikl and Bogenberger, 2015). According to Shaheen et al. (2018), more than 31 million users around the world have registered carsharing services by October 2018. Early carsharing operators provide strict round-trip carsharing services where the customers are required to pick up and drop off a vehicle at the same stations. To increase attractiveness, more flexible one-way carsharing services, which allow customers to return a vehicle at a station different from the pick-up station, have been provided. The flexibility of one-way carsharing services, however, inevitably leads to the vehicle imbalance problem across stations, i.e., the number of vehicles/parking spots available at a station does not match the customers' demand over a particular period (Barth et al., 2004; Guo et al., 2023). An effective way to cope with the vehicle imbalance issue is to relocate vehicles by a crew of dedicated fleet managing staff (Lu et al., 2022; Zakaria et al., 2018). Nevertheless, such vehicle relocation operations may result in the imbalanced distribution of staff members among stations (Yang et al., 2021; Zhao et al., 2018). Staff members need to self-rebalance by the movement among stations such that a series of relocation operations can be performed. The decision making of vehicle relocation should be jointly determined with staff rebalancing to ensure the smooth operation of one-way carsharing services (Nourinejad et al., 2015; Xu et al., 2018).

Due to modern internet technology's rapid development, the existing carsharing systems allow customers to reserve or cancel orders through the software-supporting platform whenever and wherever necessary (Yang et al., 2021). Some customers may make reservations or cancellations a long time in advance, while others may do so just one minute before the service time. This results in the inherently dynamic and uncertain nature of the customer demand in time and space, making the decision making of vehicle relocation and staff rebalancing more complicated and challenging (Boyacı et al., 2017). Furthermore, driven by the incentive programs exerted by the local government for vehicle electrification, more and more carsharing operators have adopted electric vehicles (EVs) in their carsharing systems (Ren et al., 2019). In comparison to the traditional gasoline vehicle, EV features limited driving range, frequent charging needs, and nonlinear charging profile, i.e., the state of charge (SOC) of an EV growing nonlinearly concerning the charging duration (Marra et al., 2012; Pelletier et al., 2017). Additional efforts should be made to factor in these characteristics in the decision making of

the vehicle relocation and staff rebalancing such that EVs will not get stagnant en route and the SOC of the battery follows the practical nonlinear charging profile when being charged (Xu and Meng, 2019; Xu et al., 2021). In light of the above facts, this study aims to address the real-time vehicle relocation and staff rebalancing problem for a one-way electric carsharing system while considering the demand uncertainty and practical nonlinear charging profile.

1.1. Literature review

Over the past decade, many studies have investigated the decision-making problems faced by the carsharing operators, ranking from the strategical (e.g., the locations, amounts, and parking capacities of stations), the tactical (e.g., fleet size and staff size), to the operational (e.g., vehicle relocation, staff rebalancing, and trip price) level. Readers may refer to the review articles by Illgen and Höck (2019), Golalikhani et al. (2021), and Wu and Xu (2022) for more details. Early studies considered gasoline-powered carsharing services. Recently, more and more studies focused on electric carsharing services. For example, Boyacı et al. (2017) built up a framework, which integrates multi-objective mixed-integer linear programming optimization and discrete event simulation, to determine the operational decisions of vehicle relocation and staff rebalancing in a one-way electric carsharing system with reservations. Boyacı and Zografos (2019) later extended this study by allowing temporal and spatial flexibility of customers for picking up and dropping off vehicles. Gambella et al. (2018) presented a mixed-integer linear programming model to manage the daily vehicle relocation and staff rebalancing of an electric carsharing system. Xu et al. (2018) proposed a mixed-integer nonlinear and nonconvex programming model to optimize the fleet size, trip price, vehicle relocation, and staff rebalancing subject to the elastic demand for the one-way electric carsharing services. Zhao et al. (2018) formulated a mixed-integer linear programming model to determine the allocation plan of EVs and staff members on the tactical level while considering the operational vehicle relocation and staff rebalancing decisions. Xu and Meng (2019) built up a set partitioning model incorporating the practical nonlinear charging profile for the fleet sizing problem of one-way electric carsharing services. Brandstätter et al. (2020) addressed a charging station location problem for electric carsharing systems by formulating an integer linear programming model. Huang et al. (2020) compared the efficiency of the operator-based and user-based relocation strategies by building up mixed-integer nonlinear programming models. Xu et al. (2021) developed a mixed-integer nonlinear programming model to solve the fleet sizing problem faced by one-way electric carsharing providers while taking into account vehicle relocation, vehicle charging, and battery degradation. Silva et al.

(2023) provided four mixed-integer linear programming formulations to maximize the total daily rental time in one-way electric carsharing systems.

All the above-mentioned studies assumed that customer demand is known a priori overlooking its dynamic uncertain nature and cannot guide the real-time operation of a practical carsharing system. Only a very few studies have ever addressed the operational vehicle relocation problem in an ad-hoc electric carsharing system with uncertain customer demand. Xu and Wu (2023) established a dynamic algorithmic framework based on a rolling time horizon to investigate a real-time vehicle relocation and charging optimization problem for electric carsharing services. Pantelidis et al. (2022) formulated the real-time relocation problem for a fleet of EVs as a Markov Decision Process and proposed a novel node-charge graph-based vehicle relocation policy based on cost function approximation. However, both studies neglected staff rebalancing and assumed for simplicity that a vehicle can always be relocated between two stations disregarding whether a staff member is available to perform the relocation operation. Guo et al. (2023) investigated a joint vehicle relocation, charging scheduling, and staff rebalancing problem with real-time reservations for one-way carsharing services. They model the charging of EVs with queueing method.

1.2. Research gap and contributions

To the best of our knowledge, no study has ever simultaneously factored in dynamic uncertain demand, staff rebalancing, and nonlinear charging profile of each EV for vehicle relocation problem of electric carsharing services, although it is practically relevant and significant. To bridge the research gap, we will investigate a realistic real-time vehicle relocation and staff rebalancing (RT-VR&SR) problem considering dynamic uncertain demand and practical nonlinear charging profile of each EV. The objective is to determine the strategies of vehicle relocation, vehicle charging, and staff rebalancing in an online context in pursuit of profit maximization. To achieve this objective, we will formulate the RT-VR&SR problem as a Markov Decision Process (MDP) in light of its dynamic nature and develop an efficient concurrent-scheduler-based policy. Numerical experiments have demonstrated the efficiency of the proposed policy and the developed methodology. Several significant contributions to the existing studies are summarized as follows:

- We investigate an RT-VR&SR problem considering demand uncertainty and realistic nonlinear charging profile of each EV. This problem is a novel research topic with practical significance, as it simultaneously factored in dynamic uncertain demand, staff rebalancing, and

nonlinear charging profile of each EV for vehicle relocation problem of electric carsharing services.

- An MDP formulation is developed for the proposed RT-VR&SR problem. In the MDP formulation, the notions of *activity trajectory* and *trip chain*, which explicitly describe the relocation and charging strategy of an EV and the rebalancing strategy of a staff member respectively, are utilized to express the action taken at each decision epoch.
- An efficient concurrent-scheduler-based policy is proposed for the developed MDP. A novel constrained non-dominated charging strategy (CNCS), which considers scheduling restriction of staff, is incorporated to facilitate the implementation of the policy.
- Extensive numerical experiments are conducted to assess the efficiency of the proposed policy as well as the developed methodology, to analyse the impact of staff rebalancing, and to derive managerial insights.

The remainder of this study is organized as follows. Assumptions, notations, and description of the RT-VR&SR problem are elaborated in Section 2. An MDP formulation is developed for the RT-VR&SR problem in Section 3. A concurrent-scheduler-based policy is proposed in Section 4. Section 5 conducts numerical experiments to assess the efficiency of the proposed policy as well as the developed methodology, to analyse the impact of staff rebalancing, and to explore managerial insights. Conclusions and future research directions are presented in Section 6.

2. Assumption, Notations, and Problem Description

Consider a carsharing operator who provides daily ad-hoc one-way carsharing services by managing a fleet of homogenous EVs and a crew of dedicated staff among a number of pre-determined stations located in an urban area over an operational period. Customers will reserve or cancel orders through a software-supporting platform anytime during the operational period. The orders' reservation and/or cancellation information can only be known after the customers make the corresponding operations. An EV can be picked up by a customer or relocated from one station to another by a staff member. We assume uncapacitated charging stations. EVs will remain charged as long as they are idle at stations. Every time an EV is dropped off at a station by either a customer or a staff member, the customer or the staff member will be required to connect the charging plug of this EV to a charging facility before leaving the station, if necessary. Likewise, every time an EV is picked up from a station by either a customer or a

staff member, if the EV remains charged at the station, the customer or the staff member will be required to disconnect it from the charging facility before driving it away from the station. A staff member can perform a relocation task or self-rebalance between two stations by another transportation mode (e.g., bicycle and taxi). Facing the dynamically changed order information, the carsharing operator needs to update the strategies of vehicle relocation, vehicle charging, and staff rebalancing to maximize the total profit. Kindly note that the carsharing system considered in this study is the one that allows advance reservations, which do not fixate the reservation on EVs. In the following subsections, we will elaborate on the dynamic uncertain demand, EV activity trajectory & staff trip chain, and EV nonlinear charging profile. The notations used throughout this study can be found in Appendix A.

2.1. Dynamic uncertain demand

Let \mathcal{S} denote the set of stations. Each order i is described by a quintuple $[s_i^o, s_i^d, t_i^o, t_i^d, e_i]$, where $s_i^o \in \mathcal{S}$ represents the pick-up station, $s_i^d \in \mathcal{S}$ denotes the drop-off station, t_i^o stands for the departure time from the pick-up station, t_i^d indicates the arrival time at the drop-off station, and e_i is the electricity consumption. The order i can be dynamically reserved and/or cancelled during the operational period $[0, T]$, and the reservation or cancellation information of it can only be known after the customer implements the corresponding operation through the platform. The fulfillment of the order i would generate profit represented by G_i . Nevertheless, given the limited number of EVs and staff members, the order i may be rejected, which would incur a penalty E_i . In addition, we assume without loss of generality that some orders grouped in the set \mathcal{I}_0 have been reserved before the operation.

2.2. EV activity trajectory & staff trip chain

At the beginning of the operational period, EVs grouped in the set \mathcal{V} are distributed at different stations with different initial values of SOC. The initial location and SOC of an EV $v \in \mathcal{V}$ are denoted by s_v^0 and l_v^0 , respectively. During the operational period, an EV may serve several orders, and vehicle charging and vehicle relocation may be implemented between any two adjacent orders, such as i and j , to ensure that they can be served successfully without violating the travel time and electricity consumption constraints. The travel time, the electricity consumption, and the incurred operating cost for the relocation operation from the drop-off station of the order i to the pick-up station of the order j are represented by $\tau(s_i^d, s_j^o)$,

$e(s_i^d, s_j^o)$, and $c(s_i^d, s_j^o)$ respectively. For ease of elaboration, we refer to a series of activities, e.g., under service/relocation/charging, underwent in turn by an EV as an *activity trajectory* of that vehicle. An activity trajectory illustrates a specific relocation and charging strategy of an EV and is regarded feasible if the EV can serve all the orders covered by it in time with SOC no lower than a threshold SOC_{\min} imposed by the carsharing operator. The profit of an EV activity trajectory is expressed by the difference between the profit collected from the covered orders and the incurred EV relocation cost.

Similarly, staff members grouped in the set \mathcal{F} are distributed at different stations at the beginning of the operational period. The initial location of a staff member $f \in \mathcal{F}$ is denoted by \bar{s}_f^0 . A staff member may perform several relocation tasks during the daily operation. For ease of illustration, let a quadruple $[\bar{s}_m^o, \bar{s}_m^d, \bar{t}_m^o, \bar{t}_m^d]$ describe a given relocation task m , where $\bar{s}_m^o \in \mathcal{S}$ is the origin station, $\bar{s}_m^d \in \mathcal{S}$ represents the destination station, \bar{t}_m^o denotes the departure time from the origin station, and \bar{t}_m^d stands for the arrival time at the destination station. When performing these relocation tasks, a staff member may self-rebalance between two adjacent relocation tasks, namely, m and n , by taking another transport mode so that they can be performed feasibly in terms of travel time. The travel time and the incurred cost for the rebalancing operation from the destination station of the relocation task m to the origin station of the relocation task n are denoted by $\bar{\tau}(\bar{s}_m^d, \bar{s}_n^o)$ and $\bar{c}(\bar{s}_m^d, \bar{s}_n^o)$ respectively. Without loss of generality, we assume that a staff member will immediately self-rebalance to another station for the next relocation task after completing a relocation task. We refer to a series of relocation tasks and rebalancing operations performed in turn by a staff member as a *trip chain* of that staff member. A trip chain depicts a particular rebalancing strategy for a staff member and is deemed feasible if a staff member can perform all the relocation tasks covered by it in time. The cost of a trip chain is the sum of the cost incurred by the embedded rebalancing operations.

Next, we take a small electric carsharing system with eight stations (i.e., A-H), two EVs (i.e., EV 1 and EV 2), one staff member (i.e., Staff 1), and four orders (i.e., Order 1-4) as an example to illustrate EV activity trajectory and staff trip chain. Figure 1 shows the activity trajectories for the two EVs, i.e., ‘Order 1 (from A to B) → relocation (from B to C) → charging (at C) → Order 2 (from C to D)’ (for EV 1) and ‘Order 3 (from E to F) → charging (at F) → relocation (from F to G) → Order 4 (from G to H)’ (for EV 2), and a trip chain for the staff member, i.e., ‘Task 1 (from B to C) → rebalancing (from C to F) → Task 2 (from F

to G)'. We can see that EV activity trajectories and staff trip chains couple through vehicle relocation, as the relocation operations in EV activity trajectories serve as tasks in staff trip chains. In addition, based on Figure 1, we take the activity trajectory of EV 2 as an example to further elaborate on the EV charging operations. Specifically, after the corresponding customer of Order 3 drops off EV 2 at F, the customer is required to connect the charging plug of EV 2 to a charging facility before leaving F. After Staff 1 arrives at F, S generation process of the networks taff 1 is required to disconnect EV 2 from the charging facility before relocating EV 2 from F to G.

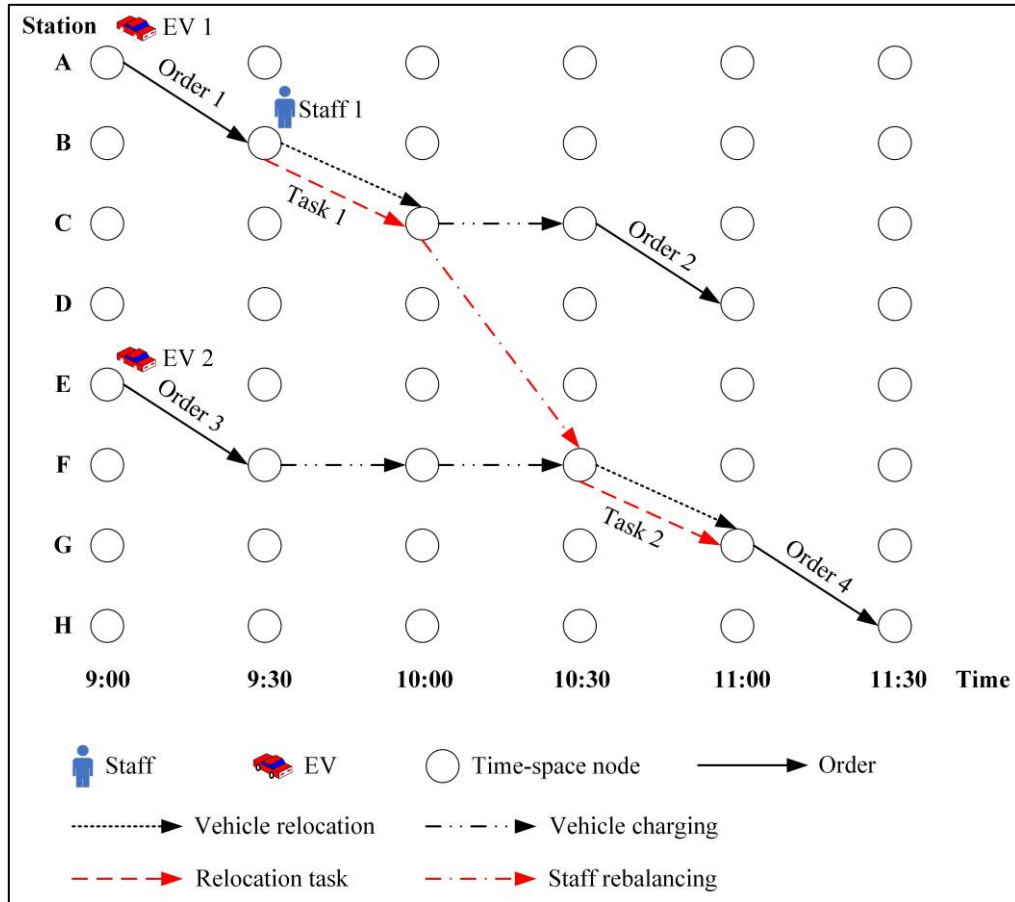


Figure 1. Illustration of vehicle relocation and staff rebalancing.

Alt Text for Figure 1: Two EVs serve four orders and each serves two, with one staff member performing two relocation tasks for the two EVs.

2.3. Nonlinear charging profile

In practical applications, a constant current-constant voltage (CC-CV) or constant power-constant voltage (CP-CV) scheme is usually adopted to charge the battery of EVs to circumvent overcharging degradation (Liu, 2013). Under both realistic charging schemes, the SOC of an

EV increases in a nonlinear manner regarding the charging duration, with the profile expressed by an implicit differential equation that has no analytical solutions (Marra et al., 2012; Pelletier et al., 2017). The temporal variations of SOC under the CC-CV and CP-CV schemes can be found in Figure 2. We can observe that the charging amount of an EV is jointly determined by the charging duration and the initial SOC before charging, as SOC does not increase at the same rate. For the convenience of illustration, the final SOC of an EV, i.e., SOC_t , after the charging duration t from the initial SOC, i.e., SOC_0 , is assumed to be determined by an implicit function $FunSOC(\bullet)$, namely:

$$SOC_t = FunSOC(t | SOC_0) \quad (1)$$

Accordingly, the duration t required to charge an EV from SOC_0 to $SOC_t \geq SOC_0$ is calculated by an implicit function $FunTime(\bullet)$ as follows:

$$t = FunTime(SOC_t | SOC_0) \quad (2)$$

The values of SOC_t and t in the above two functions can be obtained based on the numerical solution to the differential equation of the charging profile. For the details of charging profiles of EVs, the interested readers can refer to the studies of Marra et al. (2012) and Pelletier et al. (2017).

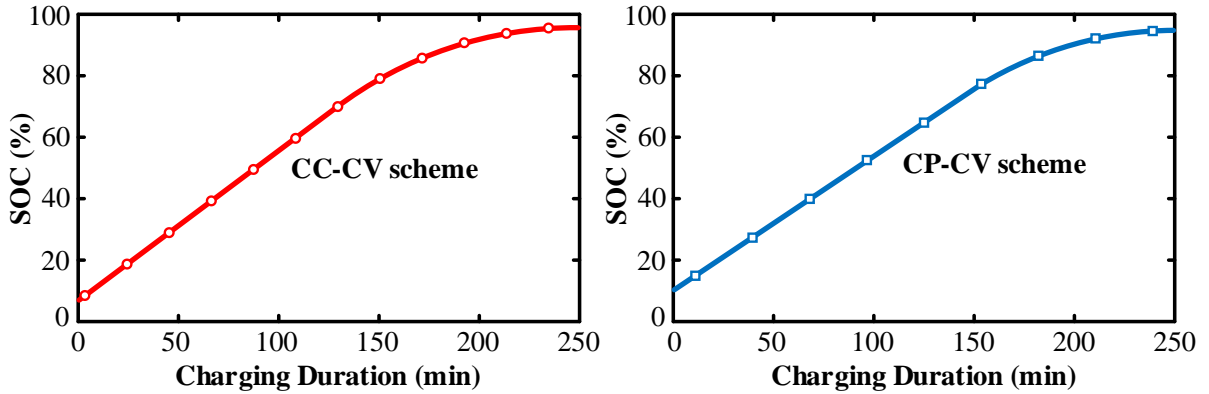


Figure 2. Illustration of nonlinear charging profiles by CC-CV and CP-CV schemes.

Alt Text for Figure 2: SOC first increases linearly and then concavely along with the rise of charging duration under the CC-CV and CP-CV charging schemes.

3. MDP Formulation

In this section, we formulate the proposed RT-VR&SR problem as an MDP, which consists of decision epochs, state space, action space, transition dynamics, rewards, and objective function. In what follows, we elaborate on these elements.

Decision epochs & state space. During the operational period $[0, T]$, a series of decision epochs are triggered in sequence by the random reservations or cancellations of customer orders. The system state at the k^{th} decision epoch triggered by an order reservation or cancellation is represented by $s_k = (V_k, F_k, \mathcal{I}_k)$, where $V_k = (V_{kv})_{v \in \mathcal{V}}$ and $F_k = (F_{kf})_{f \in \mathcal{F}}$ are vectors of EV and staff available information at the k^{th} decision epoch respectively, and \mathcal{I}_k is the set of unserved orders with departure time no earlier than the k^{th} decision epoch. The available information of each EV $v \in \mathcal{V}$ includes the earliest available time t_{kv} , available station s_{kv} , and corresponding SOC l_{kv} , i.e., $V_{kv} = (t_{kv}, s_{kv}, l_{kv})$. The available information of each staff member $f \in \mathcal{F}$ comprises the earliest available time \bar{t}_{kf} and available station \bar{s}_{kf} , i.e., $F_{kf} = (\bar{t}_{kf}, \bar{s}_{kf})$. All possible system states constitute the state space.

Action space. Given the available information of an EV $v \in \mathcal{V}$ and the set of unserved orders, i.e., V_{kv} and \mathcal{I}_k , let \mathcal{P}_{kv} denote the set of all feasible activity trajectories for the EV v . All physically real relocation tasks, i.e., the relocation tasks with different origin and destination stations, embedded in an activity trajectory $p \in \mathcal{P}_{kv}$ for an EV $v \in \mathcal{V}$ is grouped in set \mathcal{M}_{kvp} . Then $\bigcup_{v \in \mathcal{V}, p \in \mathcal{P}_{kv}} \mathcal{M}_{kvp}$ is the set of all the relocation tasks possibly implemented by staff members. Given the information of a staff member $f \in \mathcal{F}$ and the set of relocation tasks, i.e., F_{kf} and $\bigcup_{v \in \mathcal{V}, p \in \mathcal{P}_{kv}} \mathcal{M}_{kvp}$, let \mathcal{Q}_{kf} denote the set of all feasible trip chains for the staff member f . Then an action at the k^{th} decision epoch is described by $a_k = (\mathbf{x}, \mathbf{y})$, where $\mathbf{x} = (x_{vp})_{v \in \mathcal{V}, p \in \mathcal{P}_{kv}}$ is the vector of EV-trajectory decision, and x_{vp} equals 1 if the EV v implements the activity trajectory $p \in \mathcal{P}_{kv}$, and 0 otherwise; $\mathbf{y} = (y_{fq})_{f \in \mathcal{F}, q \in \mathcal{Q}_{kf}}$ is the vector of staff-chain decision and y_{fq} equals 1 if the staff member f performs the trip chain $q \in \mathcal{Q}_{kf}$, and 0 otherwise. To define the allowable actions under the system state s_k , we have the following constraints:

$$\sum_{p \in \mathcal{P}_{kv}} x_{vp} \leq 1, \quad \forall v \in \mathcal{V} \quad (3)$$

$$\sum_{v \in \mathcal{V}} \sum_{p \in \mathcal{P}_{kv}} \alpha_{vp}^i x_{vp} \leq 1, \quad \forall i \in \mathcal{I}_k \quad (4)$$

$$\sum_{q \in \mathcal{Q}_{kf}} y_{fq} \leq 1, \quad \forall f \in \mathcal{F} \quad (5)$$

$$\sum_{f \in \mathcal{F}} \sum_{q \in \mathcal{Q}_{kf}} \beta_{fq}^m y_{fq} = x_{vp}, \quad \forall v \in \mathcal{V}, p \in \mathcal{P}_{kv}, m \in \mathcal{M}_{kvp} \quad (6)$$

$$x_{vp} \in \{0,1\}, \quad \forall v \in \mathcal{V}, p \in \mathcal{P}_{kv} \quad (7)$$

$$y_{fq} \in \{0,1\}, \quad \forall f \in \mathcal{F}, q \in \mathcal{Q}_{kf} \quad (8)$$

where α_{vp}^i is the order-trajectory incidence coefficient that equals 1 if the order i is covered by activity trajectory $p \in \mathcal{P}_{kv}$, and 0 otherwise; β_{fq}^m is the task-chain incidence coefficient that equals 1 if the relocation task m is covered by a trip chain $q \in \mathcal{Q}_{kf}$, and 0 otherwise. Constraint (3) ensures that each EV implements at most one activity trajectory. Constraint (4) limits that each order is covered by at most one EV. Constraint (5) imposes that each staff member performs at most one trip chain. Constraint (6) indicates that if an EV v implements an activity trajectory $p \in \mathcal{P}_{kv}$, then each physically real relocation task embedded in the activity trajectory p will be performed by a staff member, and vice versa. Constraints (7) and (8) define the domains of decisions. All allowable actions under all possible system states from the state space form the action space.

Transition dynamics. After the k^{th} decision epoch, another random order reservation or cancellation may trigger the $(k+1)^{th}$ decision epoch and the system state transits to s_{k+1} . Let $\xi_{k+1} = (t_{k+1}, i_{k+1}, \tilde{\mathcal{J}}_{k+1})$ denote the exogenous information that becomes known at the $(k+1)^{th}$ decision epoch, where t_{k+1} is the time point of the $(k+1)^{th}$ decision epoch, i_{k+1} represents the reserved or cancelled order at the $(k+1)^{th}$ decision epoch, $\tilde{\mathcal{J}}_{k+1}$ is the set of orders with the departure time between the k^{th} and the $(k+1)^{th}$ decision epochs. Then s_{k+1} is jointly determined by the state s_k , the action a_k , and the exogenous information ξ_{k+1} through the state transition function $S^M(\bullet)$:

$$s_{k+1} = S^M(s_k, a_k, \xi_{k+1}) \quad (9)$$

In the above state transition function, the available information of an EV $v \in \mathcal{V}$ and a staff member $f \in \mathcal{F}$ at the $(k+1)^{th}$ decision epoch, i.e., $V_{(k+1)v}$ and $F_{(k+1)f}$, is determined by the available information and action at the k^{th} decision epoch, i.e., V_{kv} , F_{kf} , and a_k , and the time point of the $(k+1)^{th}$ decision epoch, i.e., t_{k+1} . Specifically, given the available information V_{kv} and F_{kf} and the action a_k , at the time point t_{k+1} , the EV v may be charging at a station, under service for an order, or in the course of relocation to another station, whereas the staff member f may be waiting at a station, performing a relocation task, or self-rebalancing to another station. We assume that an EV is available instantly if it is at a station, whereas if an EV is serving a customer or under relocation to another station, it is available only when the service or relocation operation is completed. The same also applies to staff: staff members are regarded available instantly if they are at a station; otherwise, they are deemed available only when the relocation tasks or rebalancing operations are completed. As such, the available information of the EV v and the staff member f at the $(k+1)^{th}$ decision epoch can be obtained. Regarding the set of unserved orders by the $(k+1)^{th}$ decision epoch, i.e., \mathcal{J}_{k+1} , it can be obtained by $\mathcal{J}_{k+1} = (\mathcal{J}_k \setminus \tilde{\mathcal{J}}_{k+1}) \cup \{i_{k+1}\}$ if i_{k+1} is a newly reserved order, and $\mathcal{J}_{k+1} = (\mathcal{J}_k \setminus \tilde{\mathcal{J}}_{k+1}) \setminus \{i_{k+1}\}$ otherwise.

Rewards and objective function. As a result of choosing action a_k in state s_k under a specific decision rule, a function mapping state space into action space, the carsharing operator receives a one-period reward $r_k(s_k, a_k)$. The one-period reward $r_k(s_k, a_k)$ is defined as the expected profit of the carsharing system between the k^{th} and the $(k+1)^{th}$ decision epochs and its value depends on the time point of the $(k+1)^{th}$ decision epoch, i.e., t_{k+1} . On the one hand, according to what we have discussed earlier, given the action a_k in state s_k , the time point t_{k+1} determines the available information of each EV at the $(k+1)^{th}$ decision epoch, and thus the activity trajectory of each EV from the available time at the k^{th} decision epoch to the available time at the $(k+1)^{th}$ decision epoch. Here we refer to the activity trajectory of an EV from its available time at the k^{th} decision epoch to its available time at the $(k+1)^{th}$ decision epoch as the activity trajectory of it between the k^{th} and the $(k+1)^{th}$ decision epochs. The above

expressions for activity trajectories of EVs also apply to the trip chains of staff members. On the other hand, the time point t_{k+1} determines the set of orders with the departure time between the k^{th} and the $(k+1)^{th}$ decision epochs, i.e., $\tilde{\mathcal{J}}_{k+1}$. Then the profit of the carsharing system between the k^{th} and the $(k+1)^{th}$ decision epochs can be calculated based on three terms: the profit generated from activity trajectories of EVs between the k^{th} and the $(k+1)^{th}$ decision epochs, the rebalancing cost incurred by trip chains of staff members between the k^{th} and the $(k+1)^{th}$ decision epochs, and the penalty for unserved orders in $\tilde{\mathcal{J}}_{k+1}$. Subsequently, the objective is to find a Markov policy z^* , which specifies the decision rule to be used at each decision epoch and is thus a sequence of decision rules, to maximize the expected total reward throughout the operational period by cumulating the one-period rewards:

$$\max_{z \in \mathcal{Z}} \mathbb{E}^z \left\{ \sum_{k=0}^K r_k(s_k, a_k) \mid s_0 \right\} \quad (10)$$

where \mathcal{Z} is the set of all possible Markov policies, K denotes the number of decision epochs by the end of the operational period, and $s_0 = (V_0, F_0, \mathcal{J}_0)$ represents the initial state of the carsharing system at the beginning of the operational period with $V_{0_v} = (0, s_v^0, l_v^0)$, $\forall v \in \mathcal{V}$ and $F_{0_f} = (0, \bar{s}_f^0)$, $\forall f \in \mathcal{F}$.

The formulated MDP can be solved by the traditional dynamic programming method based on the Bellman operator iterations. However, due to the three notorious curses of dimensionality, i.e., the explosion of state space, outcome space, and action space, this method can become computationally intractable even for a small-sized problem (Powell, 2007). To overcome this computational intractability, we develop an effective concurrent-scheduler-based policy for the MDP. Details are described in the next section.

4. Concurrent-scheduler-based Policy

The concurrent-scheduler-based policy is developed based on the concurrent scheduler algorithm in Xu and Meng (2019) for the joint determination of vehicle relocation and staff rebalancing strategies. For ease of illustration later, we refer to a pair of an EV and a staff member as a *combination*. In the following, we will first introduce in detail the framework for the action determination at a particular decision epoch. Then we will elaborate on the two important steps in the framework: (i) the feasibility check of a combination for serving an order

and (ii) the charging scheduling determination of the corresponding EV after the final decision of a combination has been made for serving an order. Finally, the algorithm for the action determination at a particular decision epoch will be presented.

4.1. Framework for the action determination at the k^{th} decision epoch

Take the action determination at the k^{th} decision epoch under the concurrent-scheduler-based policy as an example. Let p_{kv} and q_{kf} denote the activity trajectory implemented by an EV $v \in \mathcal{V}$ and the trip chain performed by a staff member $f \in \mathcal{F}$ at the k^{th} decision epoch, respectively. Recall that the system state at the k^{th} decision epoch is described by $s_k = (\mathbf{V}_k, \mathbf{F}_k, \mathcal{J}_k)$. To determine p_{kv} and q_{kf} , we pick the orders in \mathcal{J}_k one by one in ascending order of their departure time. For a picked order, namely, j , we first make a decision on which EV is relocated by which staff member to the pick-up station of the order j so that the order j can be served. To achieve this, for each combination of an EV in \mathcal{V} and a staff member in \mathcal{F} , we check its feasibility for serving the order j in terms of travel time and electricity consumption and calculate the incremental profit if feasible. An identified feasible combination associated with the highest and positive incremental profit to carsharing operators, namely, v^* and f^* , will be the final decision for serving the order j . Given v^* and f^* , we first determine the charging scheduling of the EV v^* for serving the order j . Then we assign the order j to the EV v^* and the corresponding relocation task, if necessary, to the staff member f^* . If there exists no such combination, the order j will not be covered by the activity trajectories implemented by EVs at the k^{th} decision epoch. Figure 3 shows the flowchart for the action determination at the k^{th} decision epoch under the concurrent-scheduler-based policy, where $\hat{\mathcal{J}}_k$ denotes the set of orders that remain to be picked and is initialized to be \mathcal{J}_k . Kindly note that the proposed concurrent-scheduler-based policy can be extended to incorporate station capacity consideration into the identification of the final combination decision for serving the order j , which can be done by checking the vehicle distribution at stations in the time dimension.

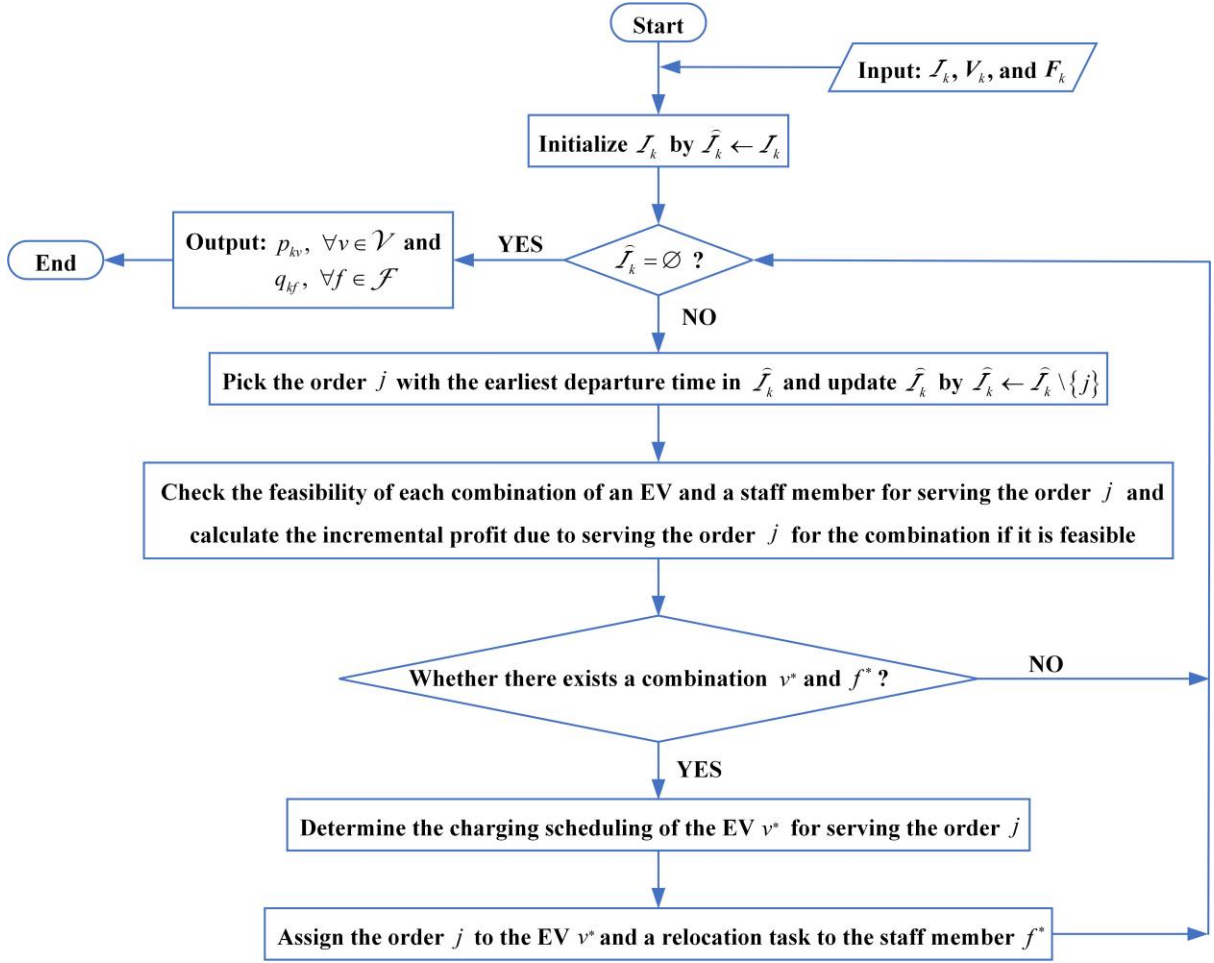


Figure 3. Flowchart for the action determination at the k^{th} decision epoch under the concurrent-scheduler-based policy.

Alt Text for Figure 3: Involved orders are assigned to a feasible combination of an EV and a staff member, which is associated with the highest and positive incremental profit, one by one in ascending order of their departure time.

Despite of the clear framework made for the action determination at the k^{th} decision epoch, the feasibility check of a combination for serving an order and the charging scheduling determination of the corresponding EV after the final decision of a combination has been made for serving an order are not easy. The intractability mainly comes from the coordination between an EV and a staff member as well as the practical nonlinear EV charging profile. In next subsection, we will elaborate on how to conduct the feasibility check of a combination for serving an order and how to determine the charging scheduling of an EV after the final decision of a combination has been made for serving an order.

4.2. Feasibility check and charging scheduling determination

As we have mentioned earlier, considering the coordination between EVs and staff members and the implicit concave charging profile, the feasibility check of a combination, v and f for example, for serving a picked order, namely j , is not straightforward. Xu and Meng (2019) proposed a non-dominated charging strategy for a pair of preceding & succeeding orders, by which the resultant SOC of an EV at the departure time of the succeeding order is not less than that by any other feasible charging strategies. Here, the charging strategy for a pair of preceding & succeeding orders refers to the charging durations at the preceding order's drop-off station and the succeeding order's pick-up station. If the non-dominated charging strategy does not exist, it implies that an EV cannot arrive at the pick-up station of the succeeding order no later than its departure time with SOC higher than or equal to SOC_{\min} . In this study, we extend the non-dominated charging strategy in Xu and Meng (2019) to a CNCS, i.e., a constrained non-dominated charging strategy, by factoring in the scheduling restriction of staff. For ease of illustration, let i_v represent the last order assigned to the EV v and $l_{i_v}^d$ be the corresponding SOC of the EV after it arrives at the drop-off station of the order i_v . If no order in \mathcal{J}_k has yet been assigned to the EV v , we assume that the last order assigned to it is a dummy one denoted by o_{kv} with the same pick-up and drop-off times at its earliest available time t_{kv} , the same pick-up and drop-off stations being its available station s_{kv} , and 0 electricity consumption. Thus, the SOC of the EV v after arriving at the drop-off station of the dummy order would be l_{kv} . In a similar vein, let m_f represent the last relocation task assigned to the staff member f . If no relocation task has yet been assigned to the staff member f , whose earliest available time and the corresponding available station are \bar{t}_{kf} and \bar{s}_{kf} respectively, a dummy relocation task denoted by \bar{o}_{kf} , with departure and arrival times being \bar{t}_{kf} and origin and destination stations being \bar{s}_{kf} , is assumed to be the last assigned relocation task. We will check the feasibility of the combination v and f for serving the order j by examining the existence of the CNCS for the pair of orders i_v and j considering the scheduling restriction of the staff member f , and verifying whether the EV v can arrive at the drop-off station of the order j with SOC no less than SOC_{\min} if the CNCS does exist. To facilitate the understanding of the following elaboration on feasibility check, Figure 4 illustrates an example of a combination of a vehicle v and a staff member f for serving the picked order j .

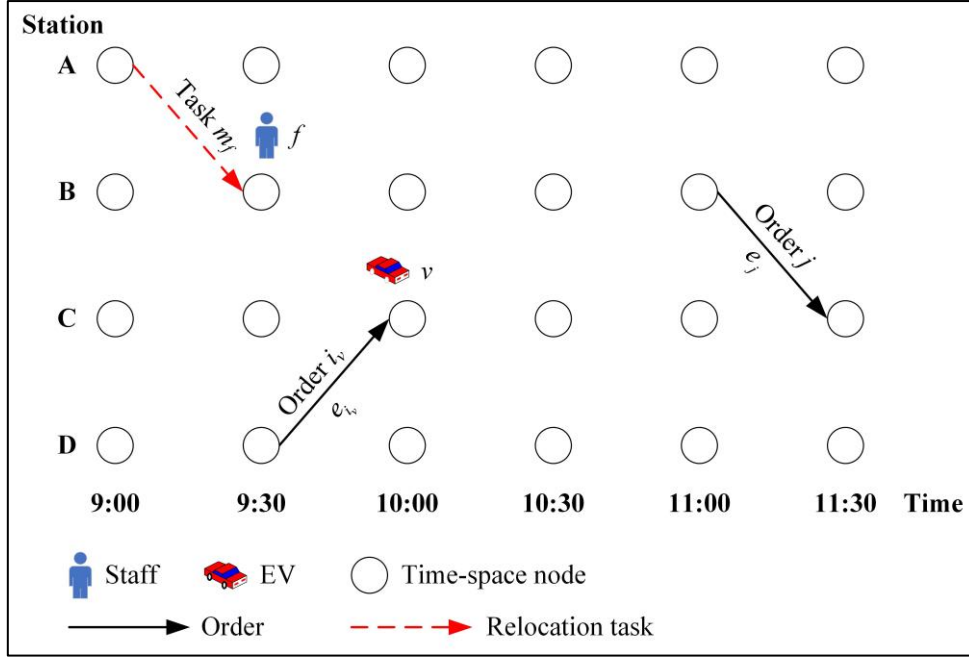


Figure 4. An example of a combination of a vehicle v and a staff member f for serving the picked order j .

Alt Text for Figure 4: An EV v , with the last assigned order being i_v , and a staff member f , with the last assigned task being m_f , are jointly to serve a picked order j .

Given the picked order j , if the combination v and f is tentatively dispatched for serving it, let Δ_{vf}^{pre} and Δ_{vf}^{suc} denote the charging durations at the drop-off station of the order i_v and the pick-up station of the order j , and l_{vf}^{suc} be the resultant SOC by the departure time of the order j . Then the feasibility check, which includes (i) the existence examination of the CNCS for the pair of orders i_v & j considering the scheduling restriction of the staff member f and (ii) the determination of the values of Δ_{vf}^{pre} , Δ_{vf}^{suc} , and l_{vf}^{suc} under the CNCS if it exists, is elaborated as follows.

Restricted by the scheduling, the EV v and the staff member f arrive at the drop-off station of the order i_v at $t_{i_v}^d$ and $\left[\bar{t}_{m_f}^d + \delta(\bar{s}_{m_f}^d, s_{i_v}^d) \right]$, respectively. Then the earliest possible time t^{elst} at which the EV v can be picked up by the staff member f for relocation is the larger one in $t_{i_v}^d$ and $\left[\bar{t}_{m_f}^d + \delta(\bar{s}_{m_f}^d, s_{i_v}^d) \right]$, i.e., $t^{elst} = \max \left\{ t_{i_v}^d, \bar{t}_{m_f}^d + \delta(\bar{s}_{m_f}^d, s_{i_v}^d) \right\}$. The corresponding SOC l^{elst} is calculated by $l^{elst} = \text{FunSOC} \left(t^{elst} - t_{i_v}^d \mid l_{i_v}^d \right)$. That is, the EV v should be charged at the

drop-off station of the order i_v for at least $\Delta_{vf}^{pre1} = t^{elst} - t_{i_v}^d$, where Δ_{vf}^{pre1} is the charging duration at the drop-off station of the order i_v until the time point t^{elst} . Then Δ_{vf}^{pre} can be determined by the charging duration at the drop-off station of the order i_v after the time point t^{elst} , i.e., Δ_{vf}^{pre2} , as it is the sum of Δ_{vf}^{pre1} and Δ_{vf}^{pre2} .

Next, the key issue is to determine Δ_{vf}^{pre2} and Δ_{vf}^{suc} that maximize l_{vf}^{suc} , if any. In fact, this is equivalent to seeking the non-dominated charging strategy for a pair of preceding & succeeding orders, where the preceding order is a dummy one with drop-off station being $s_{i_v}^d$, drop-off time at t^{elst} , and the corresponding EV SOC being l^{elst} , and the succeeding order, naturally, is the order j . Therefore, according to Xu and Meng (2019), we have the following elaboration.

(i) If $t^{elst} + \tau(s_{i_v}^d, s_j^o) > t_j^o$ or $SOC_{\max} - e(s_{i_v}^d, s_j^o) < SOC_{\min}$, the CNCS does not exist and the combination v and f is infeasible for serving the order j ; otherwise, go to step (ii) or (iii).

(ii) If $l^{elst} - e(s_{i_v}^d, s_j^o) \geq SOC_{\min}$, the CNCS exists. The EV v should be relocated directly to the pick-up station of the order j without further charging at the drop-off station of the order i_v , i.e., $\Delta_{vf}^{pre2} = 0$, and then charged at the pick-up station of the order j from $[l^{elst} - e(s_{i_v}^d, s_j^o)]$ for $\Delta_{vf}^{suc} = t_j^o - t^{elst} - \tau(s_{i_v}^d, s_j^o)$. The SOC of the EV v at the departure time of the order j under the CNCS is calculated by $l_{vf}^{suc} = FunSOC(\Delta_{vf}^{suc} | l^{elst} - e(s_{i_v}^d, s_j^o))$. The combination v and f is feasible for serving the order j only if $l_{vf}^{suc} - e_j \geq SOC_{\min}$.

(iii) If $l^{elst} - e(s_{i_v}^d, s_j^o) < SOC_{\min}$, we further need to calculate the duration required to charge the EV v from l^{elst} to $[e(s_{i_v}^d, s_j^o) + SOC_{\min}]$, i.e., $\Delta_{vf}^{pre2} = FunTime(e(s_{i_v}^d, s_j^o) + SOC_{\min} | l^{elst})$. If $t^{elst} + \Delta_{vf}^{pre2} + \tau(s_{i_v}^d, s_j^o) > t_j^o$, the CNCS does not exist and the combination v and f is infeasible for serving the order j ; otherwise, the CNCS exists, and the EV v should be relocated to the pick-up station of the order j after the charging duration Δ_{vf}^{pre2} and charged from SOC_{\min} for $\Delta_{vf}^{suc} = t_j^o - t^{elst} - \Delta_{vf}^{pre2} - \tau(s_{i_v}^d, s_j^o)$. The SOC of the EV v at the departure time of the order j under the CNCS is calculated by

$l_{vf}^{suc} = FunSOC(\Delta_{vf}^{suc} | SOC_{\min})$. The combination v and f is feasible for serving the order j only if $l_{vf}^{suc} - e_j \geq SOC_{\min}$.

Remark. If the drop-off station of the order i_v , i.e., $s_{i_v}^d$, and the pick-up station of the order j , i.e., s_j^o , are the same physical station, it can be regarded that there still exists a relocation operation for the EV v from $s_{i_v}^d$ to s_j^o , yet a dummy one that is free from the implementation of a staff member. In this way, the above elaboration on checking the feasibility of the combination v and f for serving the order j still applies, but with $t^{elst} = t_{i_v}^d$, $l^{elst} = l_{i_v}^d$, and $\Delta_{vf}^{pre1} = 0$.

If the combination v and f is feasible for serving the order j , the corresponding incremental profit $PROFIT_{vf}^{incremental}$ will be calculated by $PROFIT_{vf}^{incremental} = G_j + E_j - c(s_{i_v}^d, s_j^o) - \bar{c}(\bar{s}_{m_f}^d, s_{i_v}^d)$. In addition, given the combination v^* and f^* , we have $\Delta_{i_*}^d = \Delta_{v^*f^*}^{pre}$ and $\Delta_j^o = \Delta_{v^*f^*}^{suc}$, where $\Delta_{i_*}^d$ and Δ_j^o denote the finally determined charging durations at the drop-off station of the order i_{v^*} and the pick-up station of the order j respectively. Accordingly, a relocation task, i.e., $[s_{i_*}^d, s_j^o, t_{i_*}^d + \Delta_{i_*}^d, t_{i_*}^d + \Delta_{i_*}^d + \tau(s_{i_*}^d, s_j^o)]$, will be assigned to the staff member f^* .

4.3. Algorithm for the action determination at the k^{th} decision epoch

Algorithm 1 outlines the procedure of determining the action at the k^{th} decision epoch under the concurrent-scheduler-based policy. It should be noted that *PickEarliestOrder* is the subfunction to pick the order with the earliest departure time from the set $\hat{\mathcal{J}}_k$, and it returns the picked order and the resultant set of orders after the picking operation. *CNCS* is the subfunction to determine the CNCS when a combination v and f is dispatched for serving the order j . As discussed earlier, given the values of $t_{i_v}^d$, $l_{i_v}^d$, $\bar{t}_{m_f}^d$, $\delta(\bar{s}_{m_f}^d, s_{i_v}^d)$, $\tau(s_{i_v}^d, s_j^o)$, $e(s_{i_v}^d, s_j^o)$, and t_j^o , the charging durations at the drop-off station of the order i_v and the pick-up station of the order j , i.e., Δ_{vf}^{pre} and Δ_{vf}^{suc} , and the resultant SOC by the departure time of the order j , i.e., l_{vf}^{suc} , under the CNCS can be found if it exists; otherwise, the subfunction will

return zero as the values of Δ_{vf}^{pre} , Δ_{vf}^{suc} , and l_{vf}^{suc} . Kindly note that if the drop-off station of the order i_v/i_{v^*} and the pick-up station of the order j are the same physical station, no vehicle relocation and staff member are needed.

Algorithm 1: Pseudocode of determining the action at the k^{th} decision epoch under the concurrent-scheduler-based policy

Input: \mathcal{S}_k .

Output: p_{kv} , $\forall v \in \mathcal{V}$ and q_{kf} , $\forall f \in \mathcal{F}$.

```

1  Initialize  $\hat{\mathcal{I}}_k \leftarrow \mathcal{I}_k$ ,  $i_v \leftarrow o_{kv}$  and  $l_{i_v}^d \leftarrow l_{kv}$  for each  $v \in \mathcal{V}$ , and  $m_f \leftarrow \bar{o}_{kf}$  for each
    $f \in \mathcal{F}$ .
2  While  $\hat{\mathcal{I}}_k \neq \emptyset$  Do
3       $[j, \hat{\mathcal{I}}_k] \leftarrow \text{PickEarliestOrder}(\hat{\mathcal{I}}_k)$ ;
4      For each  $v \in \mathcal{V}$  Do
5          For each  $f \in \mathcal{F}$  Do
6               $[\Delta_{vf}^{pre}, \Delta_{vf}^{suc}, l_{vf}^{suc}] \leftarrow \text{CNCS}(t_{i_v}^d, l_{i_v}^d, \bar{t}_{m_f}^d, \delta(\bar{s}_{m_f}^d, s_{i_v}^d), \tau(s_{i_v}^d, s_j^o), e(s_{i_v}^d, s_j^o), t_j^o)$ ;
7              If  $l_{vf}^{suc} - e_j \geq \text{SOC}_{\min}$  Then
8                  If  $s_{i_v}^d \neq s_j^o$  Then
9                       $\text{PROFIT}_{vf}^{\text{incremental}} \leftarrow G_j + E_j - c(s_{i_v}^d, s_j^o) - \bar{c}(\bar{s}_{m_f}^d, s_{i_v}^d)$ ;
10                     Else  $\text{PROFIT}_{vf}^{\text{incremental}} \leftarrow G_j + E_j$ ;
11                     EndIf
12                 Else  $\text{PROFIT}_{vf}^{\text{incremental}} \leftarrow -\infty$ ;
13                 EndIf
14             EndFor
15         EndFor
16          $[v^*, f^*] \leftarrow \arg \max_{v \in \mathcal{V}, f \in \mathcal{F}} \text{PROFIT}_{vf}^{\text{incremental}}$ ;
17         If  $\text{PROFIT}_{v^* f^*}^{\text{incremental}} > 0$  Then
18              $\Delta_{i_{v^*}}^d \leftarrow \Delta_{v^* f^*}^{pre}$ ;  $\Delta_j^o \leftarrow \Delta_{v^* f^*}^{suc}$ ;
19             If  $s_{i_{v^*}}^d \neq s_j^o$  Then
20                  $m_{f^*} \leftarrow [s_{i_{v^*}}^d, s_j^o, t_{i_{v^*}}^d + \Delta_{i_{v^*}}^d, t_{i_{v^*}}^d + \Delta_{i_{v^*}}^d + \tau(s_{i_{v^*}}^d, s_j^o)]$ ;
21             EndIf
22              $i_{v^*} \leftarrow j$ ;  $l_{i_{v^*}}^d \leftarrow l_{v^* f^*}^{suc} - e_j$ ;
23         EndIf
24 EndWhile

```

5. Numerical Experiments

In this section, numerical experiments are conducted to assess the performance of the proposed concurrent-scheduler-based policy and the developed methodology, to demonstrate the necessity of staff rebalancing consideration in the decision making of vehicle relocation, and to explore the managerial insights into the operations of electric carsharing services. The algorithms are coded in C++ on a personal computer with Intel (R) Core (TM) Duo 3.0 GHz CPU. Experimental data is made publicly available at <https://github.com/TaraAtGitHub/Link-To-Instances>.

5.1. Numerical experiments on randomly generated networks

In this subsection, numerical experiments on randomly generated networks are conducted to evaluate the performance of the policy proposed for the MDP formulation and the methodology developed for the RT-VR&SR problem. The generation process of the networks and the parameter settings can be found in Appendix B.

5.1.1. Performance of the proposed policy

In the first place, we test the efficiency of the proposed concurrent-scheduler-based policy. To achieve this, we introduce a decomposition-based benchmark policy, the details of which can be found in Appendix C.

Given the total number of orders (#Demand), the number of arrivals (#Arrival), and the number of cancellations (#Cancellation) during the operational period, i.e., #Demand=300, #Arrival=200, and #Cancellation=10, different combinations of the number of stations (#Station), EVs (#EV), and staff members (#Staff), i.e., #Station $\in \{20, 40, 60\}$, #EV $\in \{40, 50, 60\}$, and #Staff $\in \{10, 20, 30\}$, are used to assess the performance of the proposed concurrent-scheduler-based policy. Ten instances are randomly generated for a particular combination and the average results are reported.

Table 1 compares the performance of the proposed concurrent-scheduler-based policy (CP) and the decomposition-based benchmark policy (DP) in terms of service level indicated by the number of satisfied orders (#SatisOrder) and profitability. We report the difference of satisfied orders (Diff_SatisOrder) and the relative increase of profit (Diff_Profit) by the proposed policy with respect to the benchmark policy. The average computation time for the action determination at each decision epoch is also reported for the two policies. The results show that both the two policies are computationally tractable in an online environment, as the longest

computation time does not exceed 1.2 seconds. For the service level and profitability, it can be seen that both the proposed policy and the benchmark policy serve fewer orders and thus obtain less profit when #Station increases. This is probably because a higher #Station would increase the diversity of spatial distribution of EVs, staff members, and orders, which may reduce the likelihood of an order being successfully served. Unlike #Station, a larger #EV, on the contrary, contributes to a higher profit by serving more orders. Regarding #Staff, its impact on service level and profitability is jointly influenced by #Station and #EV. Specifically, as #Staff increases, the proposed policy and the benchmark policy serve more orders in seven out of nine and six out of nine combinations, respectively, and both policies achieve a higher profit in eight out of nine combinations. It seems to be counter-intuitive that the profit declines slightly along with the rise of #Staff from 20 to 30 in some combinations of #Station and #EV (e.g., #Station=20 and #EV=40). This result can be attributed to the real-time and dynamic nature of the RT-VR&SR problem investigated in this study. To be more specific, in a real-time and dynamic setting, a more promising action, i.e., more promising EV activity trajectories and staff trip chains, implemented at a decision epoch under a higher #Staff, not necessarily produce a better solution over the whole operational period. As a result, the obtained profit over the whole operational period could show a downward fluctuation. The same reason can also explain the non-increasing number of satisfied orders when #Staff increases from 20 to 30 in some combinations of #Station and #EV (e.g., #Station=20 and #EV=50). As for the comparison between the proposed policy and the benchmark policy, we can see that the numbers of satisfied orders obtained by the proposed policy are higher than those achieved by the benchmark policy in most combinations of #Station, #EV, and #Staff. Besides, the proposed policy can serve as high as 18.1 orders more than the benchmark policy. In only four combinations of #Station, #EV, and #Staff, the proposed policy satisfies fewer orders than the benchmark policy by at most 1.7. In regards to the profitability, all the profits produced by the proposed policy are larger than those obtained by the benchmark policy and the largest relative gap in profit reaches 47.5% when #Station=60, #EV=40, and #Staff=10. Overall, the results demonstrate that the proposed policy outperforms the benchmark policy in solving the RT-VR&SR problem.

In addition, it is interesting to find that based on the original instance data, two multiple linear regression models can be successfully established with #SatisOrder as a function of #Station, #EV, and #Staff and Profit as a function of #Station, #EV, and #Staff. The regression results show that all of #Station, #EV, and #Staff have a significant effect on #SatisOrder and

Profit with $p < 0.001$. Besides, #Station negatively affects #SatisOrder and Profit, and #EV as well as #Staff show a positive impact on #SatisOrder and Profit, with #EV, in comparison to the other two parameters, making a much greater contribution to #SatisOrder and Profit. As a result, the regression relationship of #SatisOrder as a function of #Station, #EV, and #Staff can be represented by $\#SatisOrder = -0.45 \times \#Station + 3.06 \times \#EV + 0.37 \times \#Staff + 76.49$; the regression relationship of Profit as a function of #Station, #EV, and #Staff can be represented by $\text{Profit} = -15.60 \times \#Station + 90.77 \times \#EV + 5.23 \times \#Staff - 2059.47$.

1 Table 1. Comparison between the proposed policy and the benchmark policy based on the average results of ten randomly generated instances

#Station	#EV	#Staff	DP			CP			Comparison	
			#SatisOrder	Profit (\$)	Comp Time (s)	#SatisOrder	Profit (\$)	Comp Time (s)	Diff_SatisOrder	Diff_Profit (%)
20	40	10	194.1	1,272	0.02	195.6	1,372	0.18	1.5	7.8
20	40	20	196.2	1,295	0.02	196.9	1,378	0.33	0.7	6.4
20	40	30	196.3	1,293	0.02	196.9	1,353	0.47	0.6	4.6
20	50	10	225.2	2,194	0.02	228.0	2,340	0.30	2.8	6.7
20	50	20	232.0	2,256	0.02	231.7	2,369	0.52	-0.3	5.0
20	50	30	231.7	2,308	0.02	233.4	2,410	0.72	1.7	4.4
20	60	10	250.6	2,927	0.02	253.8	3,118	0.49	3.2	6.5
20	60	20	260.6	3,153	0.02	259.6	3,242	0.83	-1.0	2.8
20	60	30	260.6	3,199	0.02	261.0	3,276	1.13	0.4	2.4
40	40	10	174.2	776	0.02	184.2	936	0.21	10	20.6
40	40	20	186.8	820	0.02	187.9	941	0.35	1.1	14.8
40	40	30	187.6	891	0.02	187.1	956	0.50	-0.5	7.2
40	50	10	202.5	1,604	0.02	215.1	1,881	0.32	12.6	17.3
40	50	20	219.7	1,683	0.02	222.1	1,934	0.53	2.4	14.9
40	50	30	221.1	1,761	0.02	222.0	1,939	0.75	0.9	10.1
40	60	10	222.8	2,214	0.02	239.3	2,580	0.48	16.5	16.5
40	60	20	249.0	2,562	0.02	250.7	2,818	0.81	1.7	10.0
40	60	30	252.7	2,736	0.02	251.0	2,825	1.15	-1.7	3.2
60	40	10	162.9	513	0.02	175.8	757	0.24	12.9	47.5
60	40	20	179.7	642	0.02	180.4	791	0.37	0.7	23.3
60	40	30	180.3	691	0.02	181.1	793	0.52	0.8	14.8
60	50	10	190.9	1,371	0.02	206.1	1,652	0.35	15.2	20.5
60	50	20	213.2	1,539	0.02	215.1	1,731	0.55	1.9	12.5
60	50	30	213.9	1,562	0.02	216.4	1,760	0.78	2.5	12.7
60	60	10	212.9	1,988	0.03	231.0	2,421	0.52	18.1	21.8
60	60	20	242.1	2,353	0.02	244.2	2,651	0.81	2.1	12.7
60	60	30	243.5	2,437	0.02	246.1	2,685	1.14	2.6	10.2

5.1.2. Performance of the developed methodology

Subsequently, we further proceed to assess the performance of the developed methodology. Among the existing studies, Xu and Meng (2019) has developed an exact algorithm to solve a fleet size problem for one-way electric carsharing services, which considered vehicle relocation and nonlinear charging profile of EVs. Their study cannot be implemented in a real-time setting with dynamic uncertain demand but can provide an upper bound of the solution obtained by the proposed methodology. Hence, based on their study, we assess the performance of the developed methodology in a vehicle relocation (VR) problem considering practical nonlinear charging profile of each EV. Specifically, for the VR problem, we first consider the case without dynamic information ($VR^{w/o}$), where all demand information is assumed to be known in advance. We apply the developed methodology in this study and an optimality (OPT) approach adopted from the study by Xu and Meng (2019) to the problem $VR^{w/o}$. In the OPT approach, we formulate the problem $VR^{w/o}$ as a set packing model and solve it to optimality by utilizing a multi-label method. Second, based on the developed methodology, we solve the VR problem with dynamic information (VR^w), where some orders are dynamically reserved and/or cancelled during the operational period.

We test the performance of the developed methodology on instances generated from a network with 40 stations. Under each total number of orders, i.e., $\#Demand \in \{40, 60, 80, 100\}$, two numbers of arrivals, i.e., $\#Arrival/\#Demand \in \{20\%, 40\%\}$, are selected, with the number of cancellations, i.e., $\#Cancellation$, set to be zero and the number of EVs, i.e., $\#EV$, set to be 30% of $\#Demand$. Similar to Subsection 5.1.1, in addition to the number of satisfied orders, i.e., $\#SatisOrder$, and the system profit, we also report the difference in $\#SatisOrder$ and the relative variation of profit. To achieve this, for the problem $VR^{w/o}$ by the developed methodology and the problem $VR^{w/o}$ by the OPT approach, let $Diff_SatisOrder^{w/o}$ be their difference of $\#SatisOrder$ and $Diff_Profit^{w/o}$ be the relative variation in profit of the former with respect to the latter; in a similar fashion, for the problem VR^w by the developed methodology and the problem $VR^{w/o}$ by the OPT approach, let $Diff_SatisOrder^w$ be their difference of $\#SatisOrder$ and $Diff_Profit^w$ be the relative variation in profit of the former with respect to the latter. Again, ten instances are randomly generated and the average results are reported.

Table 2 shows the evaluation results on the performance of the developed methodology. It can be seen that for the comparison between the problem $VR^{w/o}$ by the developed methodology and the problem $VR^{w/o}$ by the OPT approach, the satisfied orders obtained from

the former are fewer than the latter by no more than 1 in the majority of scenarios. Particularly, under $\#Demand=100$ and $\#Arrival=20$, the former serves an equivalent number of orders as the latter. The biggest difference in the number of satisfied orders is only 1.5 when $\#Demand=60$ and $\#Arrival=12$. In terms of the system profitability, the developed methodology achieves lower profits for the problem $VR^{w/o}$ than the OPT approach in all scenarios. Nevertheless, the maximum relative decrease of profit is not higher than 10%. Regarding the comparison between the problem VR^w by the developed methodology and the problem $VR^{w/o}$ by the OPT approach, both the number of satisfied orders and profit for the former, as expected, are smaller than that for the latter in all scenarios. To be more specific, the difference in the number of satisfied orders is less than or equal to 4, and the relative decrease of profit is within 15% in more than 60% of scenarios. In addition, it seems that the relative decrease of profit declines along with the increase in the total number of orders, which may indicate the efficiency of the developed methodology in solving large-scale problem VR^w . Overall, these results demonstrate the good performance of the developed methodology.

Table 2. Evaluation results on the performance of the developed methodology

#Demand	#Arrival	Our method				OPT approach		Comparison			
		VR ^{w/o}		VR ^w		VR ^{w/o}		Diff_Satis Order ^{w/o}	Diff_Profit ^{w/o} (%)	Diff_Satis Order ^w	Diff_Profit ^w (%)
		#Satis Order	Profit (\$)	#Satis Order	Profit (\$)	#Satis Order	Profit (\$)				
40	8	38.2	500	36.9	449	38.6	533	-0.4	-6.2	-1.7	-15.8
40	16	37.6	479	35.9	417	38.5	528	-0.9	-9.3	-2.6	-21.0
60	12	57.4	755	56.8	720	58.9	835	-1.5	-9.6	-2.1	-13.8
60	24	58.1	786	55.0	684	59.0	837	-0.9	-6.1	-4.0	-18.2
80	16	78.7	1,086	77.6	1,046	79.2	1,144	-0.5	-5.0	-1.6	-8.6
80	32	78.9	1,102	75.6	989	79.4	1,151	-0.5	-4.2	-3.8	-14.1
100	20	98.6	1,399	97.3	1,359	98.6	1,448	0.0	-3.4	-1.3	-6.1
100	40	98.1	1,389	95.9	1,311	98.8	1,446	-0.7	-3.9	-2.9	-9.3

5.2. Numerical experiments on a real-world network of EVCARD

In this subsection, numerical experiments on a real-world network of EVCARD are conducted to investigate the impact of staff rebalancing and explore the effects of key parameters on the system performance. In EVCARD network, stations in three districts of Suzhou, i.e., 70 stations in Kunshan, 27 stations in Xiangcheng, and 29 stations in Wujiang, are considered. The configuration of these stations, e.g., the shortest travel time between each pair of stations, is obtained from Google Maps (Google, 2023). We combine multiple stations into one if the shortest travel time between them is within 5 min. After the combination process, 57 stations are obtained. To distinguish the transport modes by which staff members perform relocation tasks and self-rebalance, we assume that the relocation time between two stations (i.e., the shortest travel time) is X times the corresponding rebalancing time, where X is referred to as the rebalancing coefficient. Analogous to Section 5.1, ten instances of orders with $\#Demand=300$ and $\#Cancellation=10$ are randomly generated from 8 am to 6 pm, and the average results are reported. Unless stated otherwise, the reciprocal of rebalancing coefficient and the number of arrivals during the operational period, i.e., $1/X$ and $\#Arrival$, are set to be 1.4 and 200 respectively; the other parameter settings are the same as Section 5.1, which, as we have mentioned earlier, can be found in Appendix B.

5.2.1. Impact analysis of staff rebalancing

This subsection explores how staff rebalancing affects the system service level and profitability. To this end, we first consider a real-time vehicle relocation (RT-VR) problem considering demand uncertainty and nonlinear charging profile for the one-way electric carsharing services. As we have done for the proposed RT-VR&SR problem, we formulate the RT-VR problem as an MDP and solve it by the simplified concurrent-scheduler-based policy without factoring in staff rebalancing. For ease of presentation, let $\#SatisOrder^{w/o}$ and $Profit^{w/o}$ be the obtained number of satisfied orders and profit for the RT-VR problem, respectively. Accordingly, let $\#SatisOrder^w$, $Profit^{w-w}$, and $Profit^{w-w/o}$ denote the number of served orders, profit with rebalancing cost excluded, and profit without excluding rebalancing cost for the RT-VR&SR problem, respectively. The difference between $\#SatisOrder^w$ and $\#SatisOrder^{w/o}$, i.e., $Diff_SatisOrder$, and the ratio of $Profit^{w-w}$ and $Profit^{w-w/o}$ to $Profit^{w/o}$, i.e., $ProfitRatio^w$ and $ProfitRatio^{w/o}$, are adopted to evaluate the impact of staff rebalancing on the service level and profitability.

Table 3 summarizes the results under different combinations of $\#EV$ and $\#Staff$, i.e.,

$\#EV \in \{50, 55, 60\}$ and $\#Staff \in \{5, 6, 7, 8, 9, 10\}$. The results show that the number of served orders and profit with rebalancing cost excluded obtained for the RT-VR&SR problem, i.e., $\#SatisOrder^w$ and $Profit^{w-w}$, are always smaller than $\#SatisOrder^{w/o}$ and $Profit^{w/o}$ achieved for the RT-VR problem, as $Diff_SatisOrder$ is negative and the profit ratio $ProfitRatio^w$ is lower than 1. This can be explained by the fact that restricted by the availability of staff members, some relocation operations cannot be successfully performed and thus a number of orders cannot be served, which results in the loss of profit. Besides, for the RT-VR&SR problem, the profit without excluding rebalancing cost, i.e., $Profit^{w-w/o}$, is always smaller than $Profit^{w-w}$ under each combination of $\#EV$ and $\#Staff$, as a rebalancing cost term is further subtracted for $Profit^{w-w/o}$ in comparison to $Profit^{w-w}$. Naturally, the profit ratio $ProfitRatio^{w/o}$ is always lower than $ProfitRatio^w$ under each combination of $\#EV$ and $\#Staff$. The largest difference in the number of satisfied orders can be as high as 60.7 when $\#EV=60$ and $\#Staff=5$, and the corresponding profit ratios are $ProfitRatio^w=0.57$ and $ProfitRatio^{w/o}=0.52$. As $\#Staff$ increases while fleet size is constant, more relocation operations can be performed and accordingly more orders would be served, leading to the decreasing difference in the number of satisfied orders and the growing profit ratios. It is interesting to find that when fleet size increases under a constant number of staff members, the difference in the number of satisfied orders rises, whereas the profit ratio $ProfitRatio^w$ generally declines. This may indicate that expanding fleet size should be accompanied by increasing the number of staff members to earn more money by serving more orders. We can conclude from these results that staff rebalancing plays an important role in improving the service level and profitability, and ignoring it in the decision making of vehicle relocation could cause the overestimation of service level and profitability. This demonstrates the significance of this study.

Table 3. Impact of staff rebalancing on the system service level and profitability

#EV	#Staff	#Satis Order ^{w/o}	Profit ^{w/o} (\$)	#Satis Order ^w	Profit ^{w-w} (\$)	Profit ^{w-w/o} (\$)	Diff_ SatisOrder	ProfitRatio ^w (%)	ProfitRatio ^{w/o} (%)
50	5	213.1	1,789	166.2	1,065	922	-46.9	0.60	0.52
50	6	213.1	1,789	175.6	1,249	1,076	-37.5	0.70	0.60
50	7	213.1	1,789	181.2	1,360	1,164	-31.9	0.76	0.65
50	8	213.1	1,789	185.4	1,461	1,237	-27.7	0.82	0.69
50	9	213.1	1,789	194.7	1,650	1,394	-18.4	0.92	0.78
50	10	213.1	1,789	200.2	1,774	1,498	-12.9	0.99	0.84
55	5	230.2	2,284	177.1	1,383	1,239	-53.1	0.61	0.54
55	6	230.2	2,284	185.6	1,563	1,394	-44.6	0.68	0.61
55	7	230.2	2,284	193.0	1,724	1,527	-37.2	0.75	0.67
55	8	230.2	2,284	200.0	1,880	1,652	-30.2	0.82	0.72
55	9	230.2	2,284	205.2	1,980	1,731	-25.0	0.87	0.76
55	10	230.2	2,284	212.1	2,096	1,825	-18.1	0.92	0.80
60	5	246.1	2,750	185.4	1,561	1,422	-60.7	0.57	0.52
60	6	246.1	2,750	193.5	1,727	1,558	-52.6	0.63	0.57
60	7	246.1	2,750	202.2	1,960	1,765	-43.9	0.71	0.64
60	8	246.1	2,750	206.8	2,025	1,806	-39.3	0.74	0.66
60	9	246.1	2,750	214.5	2,206	1,966	-31.6	0.80	0.71
60	10	246.1	2,750	220.9	2,319	2,052	-25.2	0.84	0.75

5.2.2. Sensitivity analysis

In this subsection, we investigate how the demand dynamism, which can be indicated by the number of arrivals during the operational period, and the transport mode for staff rebalancing, which can be reflected by the reciprocal of rebalancing coefficient X , affect the performance of the one-way electric carsharing system. To conduct these numerical experiments, we assume 60 EVs and 15 staff members are provided in the carsharing system. In addition to the two concerns that the carsharing operator most cares about, i.e., the daily profit and the number of satisfied orders, several other performance indicators, i.e., the service duration per vehicle (SerDuration), the relocation duration per vehicle (RelDuration), the charging duration per vehicle (ChargeDuration), the total number of performed relocation tasks (#PerforTask), the task duration per staff member (TaskDuration), the rebalancing duration per staff member (RebDuration), and the waiting duration per staff member (WaitDuration) approximated by subtracting the sum of task and rebalancing duration from the operational period, are also reported to cater to the readers' interests. In addition, we also analyze the effects of money-related parameters, i.e., the service charge, the electricity cost (EleCost), and the rebalancing cost (RebCost), on the system performance. Details can be found in Appendix D.

Impact of demand dynamism

Since the problem focused on in this study is a real-time dynamic problem, we first explore how the demand dynamism affects the above-mentioned performance indicators. Here the demand dynamism refers to the number of orders dynamically reserved during the operational period, i.e., #Arrival, when the total number of orders considered for the RT-VR&SR problem, i.e., #Demand, and the number cancellations during the operational period, i.e., #Cancellation, are fixed. The results are shown in Table 4. We can see that when the demand dynamism increases from 20% (i.e., #Arrival=60) to 80% (i.e., #Arrival=240), both the daily profit and the number of satisfied orders decrease with fluctuations, whereas the two performance indicators decline no more than 8.5% and 4.5% respectively. This demonstrates the robustness of the proposed policy to the demand dynamism in terms of profitability and service level. On average, each EV serves about 4 orders and the carsharing operator makes a profit of around 10 \$ per order. The amounts of time allocated to each EV for serving users and relocation & charging are approximately fifty-fifty in general. As for the staff aspect, the number of performed relocation tasks is smaller than that of satisfied orders. This is consistent with our perception that fulfilling an order would generate at most one relocation task. Averagely, a staff member performs about 10 relocation tasks. Dissimilar to the time allocation

of EVs, each staff member waits at stations for more than 2.5 hours and the time spent on performing relocation tasks and self-rebalancing is comparable. The carsharing operator is suggested to improve the system efficiency by assigning tasks other than vehicle relocation, e.g., vehicle maintenance, to staff members when they stay waiting at stations.

Impact of transport mode for staff rebalancing

Last, we investigate how transport mode for staff rebalancing, which can be indicated by the reciprocal of rebalancing coefficient X , affects the performance of the one-way electric carsharing system. The results are reported in Table 5. It can be observed that both the system profitability and service level would be negatively influenced if the transport mode for rebalancing is inefficient. When the rebalancing efficiency is almost halved by increasing $\frac{1}{X}$ from 1.1 to 2, the daily profit and the number of satisfied orders decrease by 13.3% and 4.6% respectively. This is because, as shown by the results in Table 5, if the transport mode for rebalancing is less efficient, more rebalancing duration will be required, which could result in fewer relocation tasks to be performed. Consequently, a number of orders will fail to be served and thus some profits will be lost. Accordingly, as $\frac{1}{X}$ increases, staff members spend less time performing tasks and waiting at stations. Regarding the time allocation of EVs, less time is needed for service and relocation, and more time is used for charging, in general. Considering that a more efficient transport mode for rebalancing generally means a higher unit rebalancing cost, which can negatively influence the profitability and service level of the carsharing system, the operator should weigh the benefit and the cost when choosing the transport mode for rebalancing.

Table 4. Impact of demand dynamism on the performance of the one-way electric carsharing system

#Arrival	Profit (\$)	#SatisOrder	SerDuration (hr/veh)	RelDuration (hr/veh)	ChargeDuration (hr/veh)	#PerforTask	TaskDuration (hr/mem)	RebDuration (hr/mem)	WaitDuration (hr/mem)
60	2,554	247	4.79	0.86	4.24	151	3.45	3.79	2.77
80	2,563	247	4.79	0.84	4.26	148	3.38	3.70	2.93
100	2,483	243	4.73	0.86	4.28	148	3.42	3.65	2.94
120	2,484	243	4.74	0.85	4.30	150	3.40	3.79	2.81
140	2,438	241	4.71	0.84	4.38	147	3.37	3.77	2.86
160	2,354	238	4.63	0.84	4.50	146	3.35	3.69	2.96
180	2,428	239	4.67	0.83	4.51	147	3.33	3.61	3.07
200	2,377	239	4.64	0.84	4.43	147	3.35	3.57	3.08
220	2,280	235	4.57	0.84	4.55	148	3.35	3.59	3.06
240	2,338	237	4.59	0.80	4.55	143	3.21	3.30	3.49

Table 5. Impact of transport mode for staff rebalancing on the performance of the one-way electric carsharing system

1/X	Profit (\$)	#SatisOrder	SerDuration (hr/veh)	RelDuration (hr/veh)	ChargeDuration (hr/veh)	#PerforTask	TaskDuration (hr/mem)	RebDuration (hr/mem)	WaitDuration (hr/mem)
1.1	2,491	241	4.70	0.87	4.36	154	3.47	3.00	3.53
1.2	2,464	241	4.69	0.86	4.40	151	3.43	3.19	3.38
1.3	2,437	240	4.67	0.84	4.44	149	3.36	3.34	3.30
1.4	2,377	239	4.64	0.84	4.43	147	3.35	3.57	3.08
1.5	2,326	237	4.61	0.82	4.50	143	3.28	3.70	3.02
1.6	2,314	236	4.61	0.81	4.53	145	3.25	3.92	2.83
1.7	2,285	236	4.59	0.79	4.56	141	3.16	4.10	2.74
1.8	2,220	234	4.55	0.78	4.61	139	3.13	4.25	2.63
1.9	2,201	232	4.54	0.76	4.64	136	3.03	4.37	2.60
2.0	2,160	230	4.51	0.75	4.67	135	2.99	4.45	2.56

6. Conclusions

This study investigated a RT-VR&SR problem for the one-way electric carsharing services by taking into account the dynamic uncertain demand and practical nonlinear charging profile. An MDP formulation was first developed for the RT-VR&SR problem. An efficient concurrent-scheduler-based policy, which incorporates a novel CNCS, was subsequently proposed. Numerical experiments were conducted to assess the efficiency of the proposed policy and the developed methodology, to demonstrate the necessity of considering staff rebalancing in the decision making of vehicle relocation, and to explore the managerial insights of the carsharing system. The results indicated that the proposed concurrent-scheduler-based policy has an obvious advantage over the benchmark policy in solving the RT-VR&SR problem, the developed methodology shows a good performance, and ignoring staff rebalancing in the vehicle relocation problem of carsharing services will cause the overestimation of service level and profitability. In addition, the carsharing operator should well weigh the benefit and the cost when choosing the transport mode for rebalancing.

Future research can be undertaken in several aspects. First, this study assumes that the users always pick up and drop off vehicles according to the time they have reserved through the software-supporting platform. However, users are more likely to pick up and drop off vehicles within a time window containing the time epoch they have reserved. Considering the time window of orders would make the study align with reality. Second, most of the existing studies focused on either an electric or a gasoline-powered carsharing system. It would be interesting to consider a hybrid carsharing system with both electric and gasoline-powered vehicles in the future. Third, in the era of big data, adopting the data-driven approach to address the decision-making problems arising from carsharing services by utilizing massive historical data would be inevitable. Last but not least, the battery, as an essential component of an EV, has a significant impact on the profitability of a one-way electric carsharing system. On the one hand, a larger battery capacity generally means a higher EV cost. On the other hand, a larger battery capacity induces a higher electricity consumption rate; the battery capacity and the electricity consumption rate jointly influence the service capability of an EV. Hence, determining the optimal battery capacity is another crucial decision-making problem for carsharing services.

Acknowledgements

The work described in this paper was substantially supported by a grant from the Research

Grants Council of the Hong Kong Special Administrative Region, China (Project No. PolyU 25207319). We also appreciate the support from the Research Committee of The Hong Kong Polytechnic University under project code UAHJ.

References

- Barth, M., Todd, M., Xue, L., 2004. User-based vehicle relocation techniques for multiple-station shared-use vehicle systems. *Transportation Research Record* 1887, 137–144.
- Boyacı, B., Zografos, K.G., 2019. Investigating the effect of temporal and spatial flexibility on the performance of one-way electric carsharing systems. *Transportation Research Part B: Methodological* 129, 244-272.
- Boyacı, B., Zografos, K.G., Geroliminis, N., 2017. An integrated optimization-simulation framework for vehicle and personnel relocations of electric carsharing systems with reservations. *Transportation Research Part B: Methodological* 95, 214-237.
- Brandstätter, G., Leitner, M., Ljubić, I., 2020. Location of charging stations in electric car sharing systems. *Transportation Science* 54, 1408-1438.
- Gambella, C., Malaguti, E., Masini, F., Vigo, D., 2018. Optimizing relocation operations in electric car-sharing. *Omega* 81, 234-245.
- Golalikhani, M., Oliveira, B.B., Carravilla, M.A., Oliveira, J.F., Antunes, A.P., 2021. Carsharing: a review of academic literature and business practices toward an integrated decision-support framework. *Transportation Research Part E: Logistics transportation review* 149, 102280.
- Google, 2023. Google Maps. <https://www.google.com.hk/maps> (accessed 04.03.2023).
- Guo, G., Kang, M., Sun, T., 2023. Vehicle/Employee Rebalancing and Charging Scheduling in One-Way Car Sharing Systems. *IEEE Transactions on Intelligent Transportation Systems*.
- Huang, K., An, K., Rich, J., Ma, W., 2020. Vehicle relocation in one-way station-based electric carsharing systems: a comparative study of operator-based and user-based methods. *Transportation Research Part E: Logistics Transportation Review* 142, 102081.
- Illgen, S., Höck, M., 2019. Literature review of the vehicle relocation problem in one-way car sharing networks. *Transportation Research Part B: Methodological* 120, 193-204.

- Kang, K., Zhang, L., He, M., Zhang, Z., 2022. Asset-light operation strategy for car-sharing model with vertical shareholding: financial leasing or instalment factoring. *International Journal of Production Research*, 1-19.
- Li, L., Zhang, Y., 2023. An extended theory of planned behavior to explain the intention to use carsharing: a multi-group analysis of different sociodemographic characteristics. *Transportation* 50, 143-181.
- Liu, W., 2013. *Introduction to hybrid vehicle system modeling and control*. John Wiley & Sons.
- Lu, Y., Wang, K., Yuan, B., 2022. The vehicle relocation problem with operation teams in one-way carsharing systems. *International Journal of Production Research* 60, 3829-3843.
- Marra, F., Yang, G.Y., Træholt, C., Larsen, E., Rasmussen, C.N., You, S., 2012. Demand profile study of battery electric vehicle under different charging options, *2012 IEEE Power and Energy Society General Meeting*. IEEE, pp. 1-7.
- Nissan, 2023. Nissan Leaf. <http://www.nissanusa.com/electric-cars/leaf/> (accessed 04.03.2023).
- Nourinejad, M., Zhu, S., Bahrami, S., Roorda, M.J., 2015. Vehicle relocation and staff rebalancing in one-way carsharing systems. *Transportation Research Part E: Logistics and Transportation Review* 81, 98-113.
- Pantelidis, T.P., Li, L., Ma, T.-Y., Chow, J.Y., Jabari, S.E.G., 2022. A node-charge graph-based online carshare rebalancing policy with capacitated electric charging. *Transportation Science* 56, 654-676.
- Pelletier, S., Jabali, O., Laporte, G., Veneroni, M., 2017. Battery degradation and behaviour for electric vehicles: review and numerical analyses of several models. *Transportation Research Part B: Methodological* 103, 158-187.
- Powell, W.B., 2007. *Approximate dynamic programming: solving the curses of dimensionality*. John Wiley & Sons.
- Ren, S., Luo, F., Lin, L., Hsu, S.-C., Li, X.I., 2019. A novel dynamic pricing scheme for a large-scale electric vehicle sharing network considering vehicle relocation and vehicle-grid-integration. *International Journal of Production Economics* 218, 339-351.
- Shaheen, S., Cohen, A., Jaffee, M., 2018. Worldwide carsharing growth. *Transportation Sustainability Research Center, University of California, Berkeley*.

https://escholarship.org/content/qt61q03282/qt61q03282_noSplash_74ac9b5438b71e5b2f3250e6c1e14099.pdf (accessed 03.02.2023).

- Silva, W.R., Usberti, F.L., Schouery, R.C., 2023. On the complexity and modeling of the electric vehicle sharing problem. *Computers Industrial Engineering*, 109208.
- Weikl, S., Bogenberger, K., 2015. A practice-ready relocation model for free-floating carsharing systems with electric vehicles—mesoscopic approach and field trial results. *Transportation Research Part C: Emerging Technologies* 57, 206-223.
- Wu, T., Xu, M., 2022. Optimization Problems for Carsharing Service Operations: A Literature Review. *Multimodal Transportation*, under review.
- Xu, M., Meng, Q., 2019. Fleet sizing for one-way electric carsharing services considering dynamic vehicle relocation and nonlinear charging profile. *Transportation Research Part B: Methodological* 128, 23-49.
- Xu, M., Meng, Q., Liu, Z., 2018. Electric vehicle fleet size and trip pricing for one-way carsharing services considering vehicle relocation and personnel assignment. *Transportation Research Part B: Methodological* 111, 60-82.
- Xu, M., Wu, T., 2023. Real-time vehicle relocation and charging optimization for electric and shared vehicle systems. *Omega*, under 1st round review.
- Xu, M., Wu, T., Tan, Z., 2021. Electric vehicle fleet size for carsharing services considering on-demand charging strategy and battery degradation. *Transportation Research Part C: Emerging Technologies* 127, 103146.
- Yang, S., Wu, J., Sun, H., Qu, Y., Li, T., 2021. Double-balanced relocation optimization of one-way car-sharing system with real-time requests. *Transportation Research Part C: Emerging Technologies* 125, 103071.
- Zakaria, R., Dib, M., Moalic, L., 2018. Multiobjective car relocation problem in one-way carsharing system. *Journal of Modern Transportation* 26, 297-314.
- Zhao, M., Li, X., Yin, J., Cui, J., Yang, L., An, S., 2018. An integrated framework for electric vehicle rebalancing and staff relocation in one-way carsharing systems: model formulation and lagrangian relaxation-based solution approach. *Transportation Research Part B: Methodological* 117, 542-572.

Appendix A: Notations

\mathcal{S}	Set of stations
i, j	Index for an order
s_i^o	Pick-up station of the order i
s_i^d	Drop-off station of the order i
t_i^o	Departure time from the pick-up station of the order i
t_i^d	Arrival time at the drop-off station of the order i
e_i	Electricity consumption of the order i
T	Duration of the operational period
G_i	Revenue collected from the order i
E_i	Penalty for rejecting the order i
\mathcal{J}_0	Set of orders that have been reserved at the beginning of the operational period
\mathcal{V}	Set of EVs
v	Index for an EV
s_v^0	Initial location of the EV v
l_v^0	Initial SOC of the EV v
$\tau(s_i^d, s_j^o)$	Travel time for the relocation operation from the drop-off station of the order i to the pick-up station of the order j
$e(s_i^d, s_j^o)$	Electricity consumption for the relocation operation from the drop-off station of the order i to the pick-up station of the order j
$c(s_i^d, s_j^o)$	Operating cost for the relocation operation from the drop-off station of the order i to the pick-up station of the order j
SOC_{\min}	The minimum SOC allowed in the electric carsharing system
\mathcal{F}	Set of staff members
f	Index for a staff member
\bar{s}_f^0	Initial location of the staff member f
m, n	Index for a relocation task
\bar{s}_m^o	Origin station of the relocation task m
\bar{s}_m^d	Destination station of the relocation task m
\bar{t}_m^o	Departure time from the origin station of the relocation task m
\bar{t}_m^d	Arrival time at the destination station of the relocation task m
$\bar{\tau}(\bar{s}_m^d, \bar{s}_n^o)$	Travel time for the rebalancing operation from the destination station of the relocation task m to the origin station of the relocation task n
$\bar{c}(\bar{s}_m^d, \bar{s}_n^o)$	Incurring cost for the rebalancing operation from the destination station of the relocation task m to the origin station of the relocation task n
S_k	System state at the k^{th} decision epoch
\mathbf{V}_k	Vector of EV available information at the k^{th} decision epoch
V_{kv}	Available information of the EV v at the k^{th} decision epoch
\mathbf{F}_k	Vector of staff available information at the k^{th} decision epoch

F_{kf}	Available information of the staff member f at the k^{th} decision epoch
\mathcal{I}_k	Set of orders with departure time no earlier than the k^{th} decision epoch
t_{kv}	The earliest available time of the EV v at the k^{th} decision epoch
s_{kv}	The available station of the EV v at the k^{th} decision epoch
l_{kv}	The available SOC of the EV v at the k^{th} decision epoch
\bar{t}_{kf}	The earliest available time of the staff member f at the k^{th} decision epoch
\bar{s}_{kf}	The available station of the staff member f at the k^{th} decision epoch
\mathcal{P}_{kv}	Set of feasible activity trajectories for the EV v at the k^{th} decision epoch
p	Index for an EV activity trajectory
\mathcal{M}_{kvp}	Set of physically real relocation tasks embedded in the activity trajectory $p \in \mathcal{P}_{kv}$ at the k^{th} decision epoch
\mathcal{Q}_{kf}	Set of feasible trip chains for the staff member f at the k^{th} decision epoch
q	Index for a staff trip chain
a_k	Action at the k^{th} decision epoch
\mathbf{x}	Vector of EV-trajectory decisions
x_{vp}	A decision that equals 1 if the EV v implements the activity trajectory p , and 0 otherwise
\mathbf{y}	Vector of staff-chain decisions
y_{fq}	A decision that equals 1 if the staff member f performs the trip chain q , and 0 otherwise
α_v^{ip}	Order-trajectory incidence coefficient that equals 1 if order i is covered by activity trajectory $p \in \mathcal{P}_{kv}$, and 0 otherwise
β_f^{mq}	Task-chain incidence coefficient that equals 1 if relocation task m is covered by trip chain $q \in \mathcal{Q}_{kf}$, and 0 otherwise
ξ_{k+1}	Exogenous information that becomes known at the $(k+1)^{th}$ decision epoch
t_{k+1}	Time point of the $(k+1)^{th}$ decision epoch
i_{k+1}	Reserved or cancelled order at the $(k+1)^{th}$ decision epoch
$\tilde{\mathcal{I}}_{k+1}$	Set of orders with the departure time between the k^{th} and the $(k+1)^{th}$ decision epochs
$r_k(s_k, a_k)$	A reward received by the carsharing operator at the k^{th} decision epoch as a result of choosing action a_k in state s_k
\mathcal{Z}	Set of all possible Markov policies
z	Index for a Markov policy
K	Number of decision epochs before the end of the operational period
s_0	Initial system state
\mathbf{V}_0	Vector of EV initial information
V_{0v}	Initial information of the EV v

F_0	Vector of Staff initial information
F_{0f}	Initial information of the staff member f
p_{kv}	The activity trajectory implemented by the EV v at the k^{th} decision epoch
q_{kf}	The trip chain performed by the staff member f at the k^{th} decision epoch
v^* and f^*	The combination of an EV and a staff member associated with the highest and positive incremental profit
i_v	The last order assigned to the EV v
$l_{i_v}^d$	SOC of the EV v after it arrives at the drop-off station of the order i_v
o_{kv}	A dummy order with the same pick-up and drop-off stations being s_{kv} , the same pick-up and drop-off times at t_{kv} , and 0 electricity consumption
m_f	The last relocation task assigned to the staff member f
\bar{o}_{kf}	A dummy relocation task with origin and destination stations being \bar{s}_{kf} and departure and arrival times at \bar{t}_{kf}
Δ_{vf}^{pre}	Charging duration at the drop-off station of the order i_v if the combination v and f is tentatively dispatched for serving a picked order
Δ_{vf}^{suc}	Charging duration at the pick-up station of a picked order if the combination v and f is tentatively dispatched for serving the order
l_{vf}^{suc}	EV SOC by the departure time of a picked order if the combination v and f is tentatively dispatched for serving the order
t^{elst}	The earliest possible time at which the EV v is picked up by the staff member f for relocation if a combination v and f is tentatively dispatched for serving a picked order
l^{elst}	The corresponding EV SOC at the time t^{elst}
Δ_{vf}^{pre1}	Charging duration at the drop-off station of the order i_v until the time point t^{elst}
Δ_{vf}^{pre2}	Charging duration at the drop-off station of the order i_v after the time point t^{elst}
$PROFIT_{vf}^{incremental}$	Incremental profit if a combination v and f is tentatively dispatched for serving an order
$\Delta_{i_v^*}^d$	Determined charging duration at the drop-off station of the order i_{v^*}
Δ_j^o	Determined charging duration at the pick-up station of the order j
$\hat{\mathcal{J}}_k$	Set of orders that remain to be picked for assignment when determining the action at the k^{th} decision epoch

Appendix B: Supplement for network generation and parameter setup

In order to generate the random instances for the assessment of the proposed policy and the developed methodology, we build up a transportation network in a Euclidean plane of 50 km by 50 km where the travel distance between any two points is the Euclidean distance between them. To be specific, we uniformly generate $|\mathcal{S}|$ stations in the Euclidean plane. As shown in Figure 5, these stations are randomly selected from 121 candidates, each representing a vertex on a 5 km x 5 km grid. The pick-up and drop-off stations of an order i , i.e., s_i^o and s_i^d , and the initial locations of each EV $v \in \mathcal{V}$ and each staff member $f \in \mathcal{F}$, i.e., s_v^0 and \bar{s}_f^0 , are randomly chosen from these generated stations. We assume that the duration of the operational period is 10 hours. If the time duration is measured in minutes, the operational period would be $[0, 600]$. For an order i , if it is reserved before the operational period, the pick-up time t_i^o is randomly selected from the integer set $\{0, 1, 2, \dots, 600\}$ and the reservation time denoted by t_i^r is set to be a negative number, e.g., -1; otherwise, t_i^o is a random integer chosen from the set $\{1, 2, 3, \dots, 600\}$ and t_i^r is randomly generated from the integer set $\{0, 1, 2, \dots, t_i^o - 1\}$. As for an order i that is cancelled during the operational period, the cancellation time represented by t_i^c is chosen as a random integer from the set $\{t_i^r + 1, t_i^r + 2, \dots, t_i^o - 1\}$. Let $d(s_i^o, s_i^d)$ be the Euclidean distance between the pick-up station and drop-off stations of the order i , and ω_i denote its minimum duration. The average travel speed for vehicle relocation denoted by v is assumed to be 40 km/hr. If the order i is a one-way trip, which suggests that its drop-off station is different from its pick-up station, the minimum duration would be $\omega_i = d(s_i^o, s_i^d) / v$; otherwise, ω_i is set to be 40 min, as we assume there is a non-zero minimum service duration limit imposed by carsharing operators for a round-trip order to ensure the minimum profit gains. Thus, the drop-off time of the order i , i.e., t_i^d , is randomly chosen from the integer set $\{t_i^o + \omega_i, t_i^o + \omega_i + 10 \text{ min}, t_i^o + \omega_i + 20 \text{ min}, \dots, t_i^o + \omega_i + 60 \text{ min}\}$.

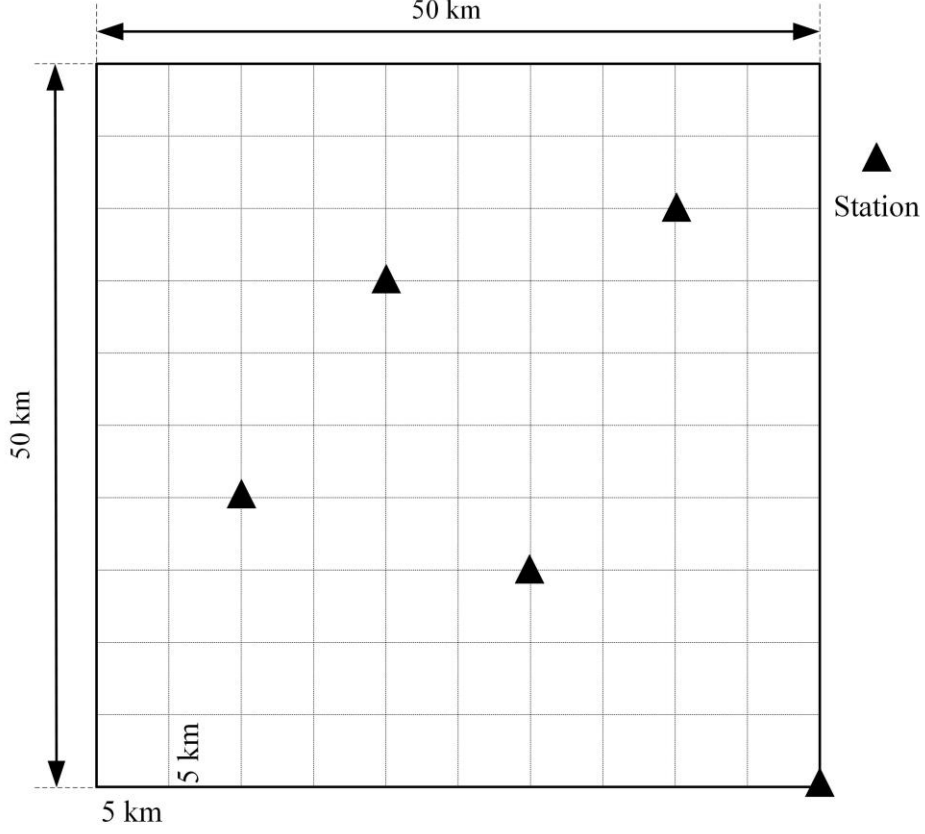


Figure 5. An illustrative example for station selection.

Alt Text for Figure 5: Several stations are randomly selected from 121 candidates in a Euclidean plane of 50 km by 50 km, each representing a vertex on a 5 km x 5 km grid.

All EVs are assumed to be equipped with a 30-kWh lithium-ion battery and charged by a CC-CV scheme. All the CC-CV charging scheme parameters are adopted from the numerical example presented by Pelletier et al. (2017). The initial SOC of all EVs is assumed to be randomly distributed between 70% and SOC_{\max} , where SOC_{\max} is the maximum value of SOC achieved by the CC-CV charging scheme. The battery's discharging rate η is set at 30%/hr (Nissan, 2023), and the minimum allowable SOC in a carsharing system, i.e., SOC_{\min} , is assumed to be 0.1. The electricity consumption of an order i , i.e., e_i , is randomly generated from the interval $[\omega_i, t_i^d - t_i^o] \times \eta$. The travel time and electricity consumption for the relocation operation from the drop-off station of an order i to the pick-up station of an order j are calculated by $\tau(s_i^d, s_j^o) = d(s_i^d, s_j^o) / v$ and $e(s_i^d, s_j^o) = \tau(s_i^d, s_j^o) \times \eta$, respectively. The rebalancing time from the destination station of a relocation task m to the origin station of a

relocation task n is calculated by $\delta(\bar{s}_m^d, \bar{s}_n^o) = d(\bar{s}_m^d, \bar{s}_n^o) / \bar{v}$, where \bar{v} is the average travel speed of the transport mode for rebalancing and is assumed to be 30 km/hr.

We assume without loss of generality that the carsharing service is charged by the service duration of orders, and the service charge is set at 0.3 \$/min. The penalty for rejecting an order is set at half of the service charge, i.e., 0.15 \$/min. The operating cost of EVs incurred by order trips and relocation trips only depends on the amount of electricity consumption, and the electricity cost is set at 0.7 \$/kWh. The rebalancing cost of staff members is set at 0.1 \$/min.

Appendix C: Supplement for the benchmark policy

To demonstrate the efficiency of the proposed policy in terms of solution quality, we further develop a decomposition-based benchmark policy. The idea of decomposition in the benchmark policy has been commonly utilized to solve the vehicle relocation and staff rebalancing problem for gasoline-powered carsharing services (Nourinejad et al., 2015; Yang et al., 2021). The benchmark policy determines the action at each decision epoch by assigning orders to EVs and relocation tasks to staff members in a separate way. That is, at each decision epoch, we attempt to obtain the activity trajectory of each EV first, and then utilize the relocation tasks embedded in the activity trajectories to determine the trip chain of each staff member. Considering that there may exist relocation tasks that staff members cannot perform due to the travel time restriction, an adjustment is likely to be made for an obtained EV activity trajectory. The notations defined in Section 4 will be used for consistency.

To be more specific, at the k^{th} decision epoch for example, given the vector of EV available information V_k and the set of orders \mathcal{J}_k , we apply a simplified **Algorithm 1** that disregards staff members to obtain the activity trajectory p_{kv} for each EV $v \in \mathcal{V}$. That is, we pick the orders in \mathcal{J}_k one by one in ascending order of their departure time. For a picked order, namely, j , we check the feasibility of each EV in \mathcal{V} for serving the order j in terms of travel time and electricity consumption and calculate the incremental profit if feasible. A feasible EV associated with the highest and positive incremental profit, namely, \bar{v}^* , will be the decision for serving the order j . Given \bar{v}^* , the charging scheduling of the EV \bar{v}^* for serving the order j will be determined based on the non-dominated charging strategy. Then the order j will be assigned to the EV \bar{v}^* . If there exists no such an EV, the order j will not be covered by the activity trajectories implemented by EVs at the k^{th} decision epoch. After the EV activity

trajectories are obtained, we attempt to obtain the trip chain q_{kf} for each staff member $f \in \mathcal{F}$ in a similar way. Specifically, we assign the physically real relocation tasks embedded in EV activity trajectories to staff members one by one. We pick the relocation task, namely, n , with the earliest departure time among the unpicked ones in the current EV activity trajectories. For the relocation task n , we examine the feasibility of each staff member to perform it and calculate the corresponding incremental cost if feasible. The relocation task n will be assigned to a feasible staff member with the lowest incremental cost \bar{f}^* .

However, \bar{f}^* may not exist because it is likely that no staff member is feasible to perform the task n . In other words, the inequality $\bar{t}_{m_f}^d + \delta(\bar{s}_{m_f}^d, \bar{s}_n^o) \leq \bar{t}_n^o$ may not hold for each $f \in \mathcal{F}$ and the EV in the task n cannot be relocated accordingly. In this case, an adjustment is made for the activity trajectory of the EV in the task n . For ease of illustration, let v_n denote the EV that is relocated in the task n , i_n^{pre} and i_n^{suc} be the preceding and succeeding orders that the task n connects in the activity trajectory p_{kv_n} respectively. Since the task n cannot be performed due to that the inequality $\bar{t}_{m_f}^d + \delta(\bar{s}_{m_f}^d, \bar{s}_n^o) \leq \bar{t}_n^o$ cannot hold for each $f \in \mathcal{F}$, we consider delaying the departure time of the task n , i.e., \bar{t}_n^o , by extending the charging duration of the EV v_n at the drop-off station of the order i_n^{pre} , i.e., $s_{i_n^{pre}}^d$ (\bar{s}_n^o). To achieve this, we first identify the staff member that is most likely to ensure that the EV v_n can serve the order i_n^{suc} feasibly in terms of travel time and electricity consumption. Let f^\times denote the staff member and f^\times would be the one that arrives at the origin station of the task n , i.e., \bar{s}_n^o ($s_{i_n^{pre}}^d$), at the earliest time, i.e., $f^\times := \arg \min_{f \in \mathcal{F}} (\bar{t}_{m_f}^d + \delta(\bar{s}_{m_f}^d, \bar{s}_n^o))$. Limited by the scheduling of the staff member f^\times , the charging of the EV v_n at the drop-off station of the order i_n^{pre} will be extended to the time $\bar{t}_{m_{f^\times}}^d + \delta(\bar{s}_{m_{f^\times}}^d, \bar{s}_n^o)$. With this restriction, we need to recheck the feasibility of the EV v_n to serve the succeeding order i_n^{suc} . If it is feasible, the charging durations of the EV v_n at the drop-off station of the order i_n^{pre} and the pick-up station of the order i_n^{suc} will be adjusted, and the relocation task n will be assigned to the staff member f^\times after the departure and arrival times of it are delayed accordingly; otherwise, the order i_n^{suc} will be removed from the activity

trajectory p_{kv_n} . No matter what the result is, either the charging durations are adjusted or the order i_n^{suc} is removed, the change made to the activity trajectory p_{kv_n} requires us to update the remaining activity trajectory. To achieve this, when the EV v_n attempts to depart from the drop-off station of the order i_n^{suc} (for the case that charging durations are adjusted) or the order i_n^{pre} (for the case that the order i_n^{suc} is removed) to serve a succeeding order, we should check its feasibility. If it is infeasible, the succeeding order will be removed from the activity trajectory p_{kv_n} , and the next adjacent order will be checked until all the orders have been examined.

Subsequently, we pick the next relocation task with the earliest departure time among the unpicked ones in the current EV activity trajectories, and we repeat the above process until no relocation task remains to be picked for assignment. The flowchart for the action determination at the k^{th} decision epoch under the decomposition-based policy is shown in Figure 6.

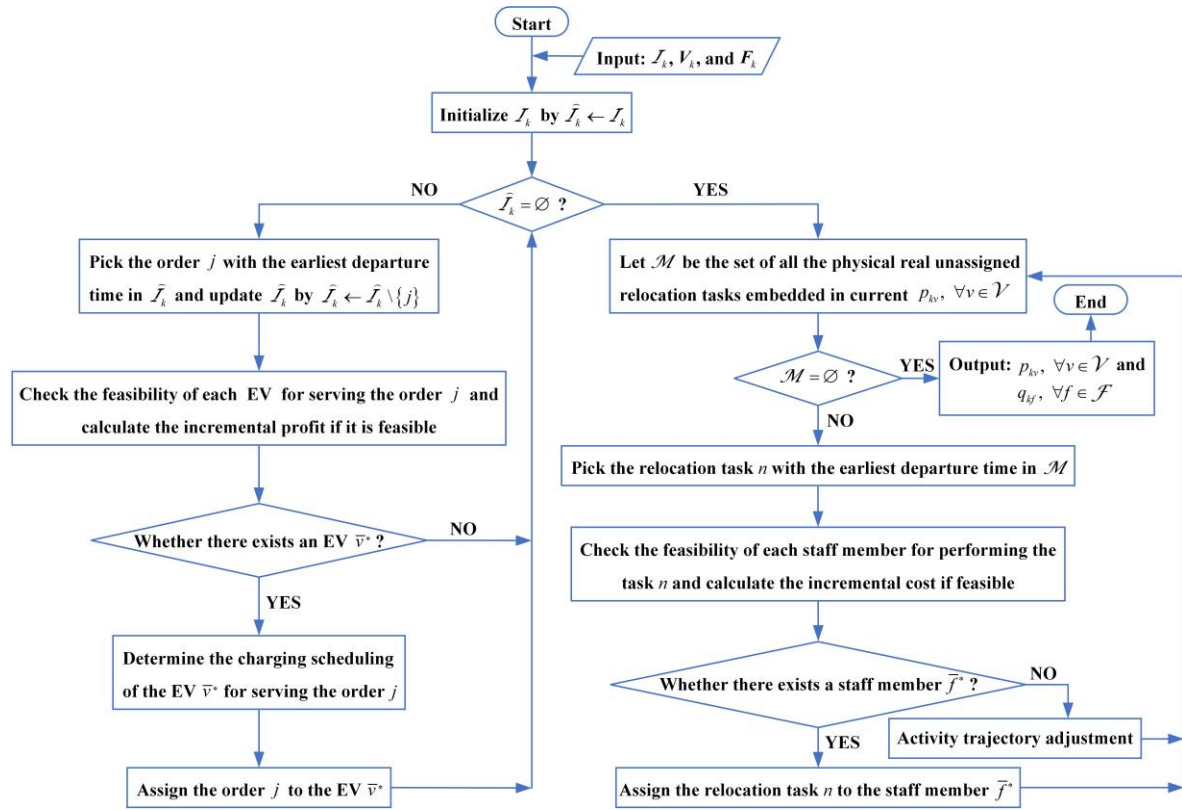


Figure 6. Flowchart for the action determination at the k^{th} decision epoch under the decomposition-based policy.

Alt Text for Figure 6: Involved orders are first assigned to EVs, and then relocation tasks embedded in EV activity trajectories are assigned to staff members, possibly along with EV activity trajectory adjustment.

Appendix D: Supplement for sensitivity analysis

Impact of service charge

We investigate the effect of the service charge on the performance of the one-way electric carsharing system. The results are presented in Table 6. It shows that if the service charge is below 0.18 \$/min, the carsharing company would be in the red¹. Setting a larger service charge makes the orders more profitable, and the carsharing operator begins to earn money. As the service charge increases from 0.03 \$/min to 0.30 \$/min with an increment of 0.03, the variation amplitude from 0.03 \$/min to 0.06 \$/min is the largest for all the performance indicators excluding the daily profit. When the service charge is higher than 0.12 \$/min, some of the performance indicators, e.g., #SatisOrder, remain almost stable with respect to the service charge. This is because if the service charge is relatively low, e.g., 0.03 \$/min, limited by that only a feasible combination of an EV and a staff member with the maximum and positive profit increment can be dispatched for serving an order, some orders may be rejected due to the negative profit increments of all feasible combinations of an EV and a staff member. When the service charge is increased to 0.06 \$/min, these negative profit increments may become positive, resulting in the visible growth of the number of satisfied orders and thus the relatively obvious variations of other performance indicators. If the service charge is high enough, e.g., 0.15 \$/min, the profit increment exerts little influence on the fulfillment of orders, and then the performance indicators generally show less sensitivity to the variation of service charge. These results indicate that under the adopted concurrent-scheduler-based policy, the carsharing operator should set the service charge higher than 0.12 \$/min to circumvent unnecessary service level drop brought by the profit increments of combinations of an EV and a staff member.

Impact of electricity cost

We also examine the effect of electricity cost on the performance of the one-way electric carsharing system. Table 7 summarizes the results. As expected, it demonstrates the significant impact of electricity cost on the profitability of the carsharing system. If the unit electricity cost

¹ The profit can be negative due to the penalty for unserved orders.

is higher than 1.7 \$, the carsharing operator would be at a loss. A notable phenomenon is that the variations of all EV-related and staff-related performance indicators appear arbitrary when the unit electricity cost is no more than 1.5 \$. However, when the unit electricity cost is larger than 1.5 \$, a higher value of it leads to a smaller number of satisfied orders, lower service and relocation durations, and thus higher charging duration. Accordingly, the number of relocation tasks performed by staff members and the task duration decrease visibly, while the rebalancing duration fluctuates, resulting in the increasing waiting duration. For these obtained results, we guess that the increase of the unit electricity cost from 0.3 \$ to 1.5 \$ probably influences the assignment decision of orders, as a feasible combination of an EV and a staff member with the maximum and positive profit increment, which includes the electricity-related terms, is the final decision for serving an order. The change in the assignment decisions of orders eventually alters activity trajectories of EVs and trip chains of staff members over the whole operational period, causing the arbitrary variations of the performance indicators. If the unit electricity cost is further increased, the profit increments of all feasible combinations of an EV and a staff member may turn negative for some orders, leading to the declining number of satisfied orders concerning unit electricity cost and the corresponding variations of other performance indicators. Hence, it should be understood by the carsharing operator that if the proposed concurrent-scheduler-based policy is adopted, unit electricity cost no larger than 1.5 \$ will exert little impact on the system service level.

Impact of rebalancing cost

We further test the variations of the performance indicators concerning the rebalancing cost. Table 8 tabulates the results. We can see that compared to the electricity cost, the rebalancing cost has a more significant impact on the system service level, as the number of satisfied orders decreases by more than 25% when the unit rebalancing cost increases from 0.1 \$ to 1.9 \$. The declining number of satisfied orders leads to fewer relocation tasks performed by staff members. As a result, all the time-related performance indicators excluding the charging and waiting durations generally decrease when the unit rebalancing cost rises. An interesting phenomenon is that the profit, instead of keeping falling with the growth of unit rebalancing cost, drops first and then increases. When the unit rebalancing cost is increased from 1.7 \$ to 1.9 \$, the carsharing system dramatically turns from loss to profit. For this result, we caution that the net profit of the carsharing system is determined by two variable terms, i.e., the total profit generated from the activity trajectories, including the penalty for unserved orders, and the total rebalancing cost incurred by the trip chains. When the unit rebalancing

cost increases, the total profit generated from the activity trajectories of EVs would normally decrease due to the falling number of satisfied orders. Nevertheless, the variation of the total rebalancing cost incurred by the trip chains of staff members, which is the product of unit rebalancing cost and rebalancing duration, is uncertain in light of the declining rebalancing duration. Hence, if the total rebalancing cost reduces and the reduction magnitude is greater than that of the total profit produced by the activity trajectories of EVs, the net profit of the carsharing system would grow. This has been confirmed by experimental data.

Table 6. Impact of service charge on the performance of the one-way electric carsharing system

Charge (\$/min)	Profit (\$)	#SatisOrder	SerDuration (hr/veh)	RelDuration (hr/veh)	ChargeDuration (hr/veh)	#PerforTask	TaskDuration (hr/mem)	RebDuration (hr/mem)	WaitDuration (hr/mem)
0.03	-2,076	230	4.59	0.78	4.53	139	3.11	3.03	3.86
0.06	-1,590	236	4.65	0.81	4.44	145	3.23	3.31	3.46
0.09	-1,098	238	4.66	0.83	4.44	147	3.30	3.36	3.34
0.12	-621	238	4.65	0.85	4.43	146	3.39	3.44	3.18
0.15	-96	240	4.68	0.84	4.43	148	3.36	3.49	3.15
0.18	405	239	4.67	0.83	4.44	147	3.31	3.51	3.19
0.21	882	239	4.66	0.84	4.45	147	3.36	3.60	3.04
0.24	1,375	239	4.65	0.84	4.45	147	3.38	3.58	3.05
0.27	1,881	239	4.65	0.84	4.43	148	3.35	3.57	3.08
0.30	2,377	239	4.64	0.84	4.43	147	3.35	3.57	3.08

Table 7. Impact of electricity cost on the performance of the one-way electric carsharing system

EleCost (\$/kWh)	Profit (\$)	#SatisOrder	SerDuration (hr/veh)	RelDuration (hr/veh)	ChargeDuration (hr/veh)	#PerforTask	TaskDuration (hr/mem)	RebDuration (hr/mem)	WaitDuration (hr/mem)
0.3	3,264	237	4.60	0.91	4.41	146	3.64	3.64	2.72
0.5	2,909	240	4.68	0.83	4.45	147	3.34	3.54	3.13
0.7	2,377	239	4.64	0.84	4.43	147	3.35	3.57	3.08
0.9	1,897	239	4.65	0.84	4.45	147	3.36	3.58	3.07
1.1	1,494	241	4.72	0.78	4.46	151	3.13	3.99	2.88
1.3	996	239	4.68	0.76	4.48	148	3.04	3.88	3.08
1.5	522	237	4.68	0.77	4.47	148	3.07	3.88	3.05
1.7	52	236	4.68	0.76	4.48	148	3.03	3.85	3.13
1.9	-425	232	4.63	0.73	4.55	145	2.90	3.88	3.22
2.1	-793	228	4.61	0.67	4.67	139	2.66	3.46	3.88

Table 8. Impact of rebalancing cost on the performance of the one-way electric carsharing system

RebCost (\$/min)	Profit (\$)	#SatisOrder	SerDuration (hr/veh)	RelDuration (hr/veh)	ChargeDuration (hr/veh)	#PerforTask	TaskDuration (hr/mem)	RebDuration (hr/mem)	WaitDuration (hr/mem)
0.1	2,377	239	4.64	0.84	4.43	147	3.35	3.57	3.08
0.3	1,683	236	4.60	0.89	4.43	146	3.57	3.47	2.96
0.5	1,164	234	4.57	0.87	4.47	142	3.47	3.18	3.35
0.7	645	229	4.48	0.84	4.56	138	3.37	2.92	3.72
0.9	426	227	4.47	0.81	4.60	130	3.23	2.54	4.23
1.1	123	218	4.30	0.75	4.80	122	3.00	2.18	4.83
1.3	-53	212	4.19	0.70	4.95	113	2.79	1.89	5.32
1.5	-170	206	4.09	0.62	5.10	100	2.48	1.65	5.87
1.7	-63	194	3.85	0.53	5.35	84	2.11	1.20	6.70
1.9	95	178	3.50	0.41	5.78	67	1.62	0.74	7.64